NACA RM L51A10

RESEARCH MEMORANDUM

AN INVESTIGATION OF THE EFFECT OF VERTICAL-FIN LOCATION AND AREA ON LOW-SPEED LATERAL STABILITY DERIVATIVES OF A SEMITAILLESS AIRPLANE MODEL

By Lewis R. Fisher and William H. Michael, Jr.

Langley Aeronautical Laboratory
Langley Field, Va.

NATIONAL ADVISORY COMMITTEE
FOR AERONAUTICS

WASHINGTON

March 7, 1951

NATIONAL ADVISORY COMMITTEE FOR AERONAUTICS

RESEARCH MEMORANDUM

AN INVESTIGATION OF THE EFFECT OF VERTICAL-FIN LOCATION AND AREA ON LOW-SPEED LATERAL STABILITY DERIVATIVES OF A SEMITAILLESS AIRPLANE MODEL

By Lewis R. Fisher and William H. Michael, Jr.

SUMMARY

The results of a low-speed wind-tunnel investigation to determine the effects of vertical-fin location and area on the static and rotary lateral stability characteristics of a semitailless airplane model indicated that the contributions of the vertical fin to the stability derivatives could be estimated with reasonable accuracy by simple considerations in spite of the unusually short tail length and large tail height of this configuration.

Although the differences in fin effectiveness are not large, for comparable fin areas and equal tail lengths, fins located at the 86-percent spanwise location are, in general, more satisfactory for providing directional stability and damping in yaw than fins located at the 43-percent spanwise location. In the low lift-coefficient region, a single central fin provided more directional stability but less damping in yaw than twin fins located at either outboard position. The central fin has an advantage over the outboard fins in that the fin effectiveness tends to increase slightly at high lift coefficients, while the trend is for the outboard fins to suffer a decrease in effectiveness in this lift-coefficient region.

Changes in vertical-fin arrangement had no appreciable effect on the damping in roll but, in some cases, resulted in significant changes in the yawing moment due to rolling.

The nature of the span loadings induced on the wing by the lift on the fins in sideslip resulted in a change of sign of the effective-dihedral parameter with lateral movement of the fins. The increment to the effective dihedral due to the vertical fins was negative at the 43-percent spanwise position and positive at the 86-percent position.

INTRODUCTION

Considerable interest has been shown in tailless airplanes because of the low drag advantages of such a design. With the advent of the use of sweepback in high-speed airplanes, this interest has heightened because a swept wing offers an effective tail length for the placement of longitudinal and directional control devices. Furthermore, removing the tail surfaces from the wake region of the wing eliminates certain adverse effects of compressibility in high-speed airplanes. A completely tailless design, however, has certain disadvantages - one being the lack of directional stability. The addition of vertical fins for the purpose of increasing the directional stability results in an arrangement which will be referred to in the present paper as a semitailless design.

The calculation of the dynamic stability of most semitailless airplanes has involved some degree of uncertainty because of the unusually short tail lengths and large tail heights of such designs. In order to establish the validity of the application of the usual methods for predicting the stability derivatives of such airplanes and to establish a basis for estimating the effects of fin area and location on these derivatives, a representative model of a semitailless airplane was tested in straight, yawing, and rolling flow in the Langley stability tunnel. This investigation was undertaken as part of an extensive program being carried out in the Langley stability tunnel to establish the effects of systematic changes in configuration upon the low-speed static and rotary stability characteristics of high-speed airplane designs.

SYMBOLS

The data presented herein are in the form of standard NACA coefficients of forces and moments which are referred to the stability system of axes (fig. 1) with the origin at 20.2 percent of the mean aerodynamic chord of the model tested. The coefficients and symbols are defined as follows:

A	aspect ratio (b^2/S)
α	angle of attack, degrees
b	wing span, feet
c	wing chord, feet

$\bar{c}$	wing mean aerodynamic chord, feet $\left(\frac{2}{S}\int_0^{b/2} c^2 db\right)$
l_t	tail length, feet
Λ_{LE}	angle of sweepback of wing leading edge, degrees
λ	taper ratio
p	rolling angular velocity, radians per second
$\frac{pb}{2V}$	rolling-velocity parameter
ψ	angle of yaw, degrees
q	dynamic pressure, pounds per square foot $\left(\frac{1}{2}\rho V^2\right)$
r	yawing angular velocity, radians per second
$\frac{rb}{2V}$	yawing-velocity parameter
ρ	mass density of air, slugs per cubic foot
S	wing area, square feet
V	free-stream velocity, feet per second
y	spanwise distance from plane of symmetry to vertical fin, feet
C_L	lift coefficient $\left(\frac{\text{Lift}}{qS}\right)$
C_D	drag coefficient $\left(\frac{\text{Drag}}{qS}\right)$
C_l	rolling-moment coefficient $\left(\frac{\text{Rolling moment}}{qSb}\right)$
C_m	pitching-moment coefficient $\left(\frac{\text{Pitching moment}}{qS\bar{c}}\right)$
C_n	yawing-moment coefficient $\left(\frac{\text{Yawing moment}}{qSb}\right)$

C_X longitudinal-force coefficient $\left(\frac{\text{Longitudinal force}}{qS}\right)$

C_Y lateral-force coefficient $\left(\frac{\text{Lateral force}}{qS}\right)$

$$C_{Y_\psi} = \frac{\partial C_Y}{\partial \psi} \qquad C_{Y_r} = \frac{\partial C_Y}{\partial\left(\frac{rb}{2V}\right)} \qquad C_{Y_p} = \frac{\partial C_Y}{\partial\left(\frac{pb}{2V}\right)}$$

$$C_{n_\psi} = \frac{\partial C_n}{\partial \psi} \qquad C_{n_r} = \frac{\partial C_n}{\partial\left(\frac{rb}{2V}\right)} \qquad C_{n_p} = \frac{\partial C_n}{\partial\left(\frac{pb}{2V}\right)}$$

$$C_{l_\psi} = \frac{\partial C_l}{\partial \psi} \qquad C_{l_r} = \frac{\partial C_l}{\partial\left(\frac{rb}{2V}\right)} \qquad C_{l_p} = \frac{\partial C_l}{\partial\left(\frac{pb}{2V}\right)}$$

APPARATUS AND TESTS

The curved-flow and the rolling-flow test equipment of the Langley stability tunnel (references 1 and 2, respectively) were utilized in obtaining the yawing and rolling characteristics of the model. By means of this equipment, the flow of air may be directed in either a curved or a rolling path past the model to simulate yawing or rolling flight. All forces and moments were measured about the 20.2-percent point of the mean aerodynamic chord of the wing of the model by a conventional six-component balance system.

The model tested was a separable wing and fuselage combination which could be tested with vertical fins placed at two different longitudinal and three different lateral locations as shown in figure 2. Tests were made of the wing alone, the wing and fuselage, and the wing and fuselage with each of the eight different vertical-fin arrangements. The following notation is used to describe the vertical-fin configurations:

V(a'L) single large fin, $\frac{y}{b/2} = 0$, $\frac{l_t}{\bar{c}} = 1.20$

V(aL) single large fin, $\frac{y}{b/2} = 0$, $\frac{l_t}{\bar{c}} = 0.85$

V(b2S) two small fins
V(b2L) two large fins
V(b4S) four small fins

$\frac{y}{b/2} = 0.43$, $\frac{l_t}{\bar{c}} = 0.85$

V(c2S) two small fins
V(c2L) two large fins
V(c4S) four small fins

$\left.\begin{matrix} \\ \\ \\ \end{matrix}\right\} \frac{y}{b/2} = 0.86, \quad \frac{l_t}{\bar{c}} = 0.85$

A single centrally located vertical fin was investigated at positions for which the fin aerodynamic center was at distances of $0.85\bar{c}$ and $1.20\bar{c}$ (positions a and a', respectively) behind the assumed origin of axes. With a tail length equal to $0.85\bar{c}$, vertical fins were also investigated at spanwise distances of $0.43\frac{b}{2}$ and $0.86\frac{b}{2}$ (positions b and c, respectively) from the plane of symmetry of the model.

The lateral positions a, b, and c all have the same tail length, which is four inches ($0.35\bar{c}$) shorter than the tail length for position a'. The plan-form area of each small fin is one-half that of each large fin. Therefore, the vertical-tail arrangements V(a'L), V(aL), V(b2S), and V(c2S) all have the same area, which is one-half that for the arrangements V(b2L), V(c2L), V(b4S), and V(c4S). For the V(b4S) and V(c4S) configurations, two additional small fins were placed on the bottom surface of the wing opposite to and in the same plane as fins V(b2S) and V(c2S), respectively.

The symbols refer to the complete model having the specific fin arrangement tested. In figures illustrating the effects of the addition of various component parts, the symbol W refers to the isolated wing and the symbol WF refers to the wing-fuselage combination. The arrangement V(a'L) is considered to be the basic configuration. Photographs of the model mounted in the Langley stability tunnel with three different fin arrangements are shown in figure 3.

The effects of the addition to the basic configuration of a cockpit canopy and wing-root engine nacelles (fig. 2) were determined in the investigation. The basic model was also tested with the addition of full-span slats attached to the leading edge of the wing. These slats were shaped from $\frac{1}{16}$-inch aluminum sheet to the contour of the wing leading edge. The V(b2L) fin arrangement was tested, with and without a pair of dorsal fins (made from $\frac{1}{8}$-inch aluminum sheet) which extended to the leading edge of the wing, primarily for the purpose of determining the effect of the dorsal fins on the damping in yaw of the model. The area of the dorsal fins was 40 percent of the area of the large vertical fins.

Test conditions are tabulated in the following table:

	Straight and yawing flow	Rolling flow
Dynamic pressure, pounds per square foot	24.9	39.8
Test Reynolds number, (based on $\bar{c}$)	900,000	1,138,000
Mach number	0.13	0.16
Yawing-velocity parameter, $\frac{rb}{2V}$	0, -0.0348, -0.0738, -0.0971	
Rolling-velocity parameter, $\frac{pb}{2V}$		$\pm$0.0227, $\pm$0.0453, $\pm$0.0680

CORRECTIONS

Corrections for the effect of jet boundaries, based on unswept-wing theory, have been applied to the angle-of-attack, longitudinal-force-coefficient, and rolling-moment-coefficient data. The data obtained in curved flow have also been corrected for the buoyancy effect of the static-pressure gradient associated with curved flow (see reference 1).

No corrections have been made for the effects of blocking, turbulence, support-strut interference, or static-pressure gradient on the boundary-layer flow.

RESULTS AND DISCUSSION

Straight Flow

Longitudinal characteristics.- The lift-curve slope of the wing alone as shown in figure 4(a) is 0.053 per degree, which is in agreement with the value predicted by reference 3. The addition of a fuselage or a fuselage and vertical fin did not affect the lift-curve slope, but a small decrease in the maximum lift and in the angle at which maximum lift occurs took place with the addition of the fuselage.

The wing and the complete model exhibit stable pitching moments through the lift-coefficient range including the stall. The wing aerodynamic center varies between $0.24\bar{c}$ at zero lift and $0.31\bar{c}$ at $C_L = 0.4$. Reference 3 predicts an aerodynamic center at $0.25\bar{c}$ for the wing.

The maximum lift coefficient for the basic model appears to be relatively low. Tests have indicated that, for a smooth wing, higher Reynolds numbers will delay the onset of partial separation of flow from the wing and will increase the maximum lift. In general, the effects of an increase in Reynolds number have been observed to be somewhat similar to the effects which result from the addition of a slat at a low Reynolds number. The characteristics of the present model with wing slats were determined, therefore, primarily for the purpose of obtaining an indication of trends that might be expected to result from increased Reynolds number. The results obtained for the longitudinal characteristics (fig. 4(b)) show that the slats tended to straighten and extend the lift curve and reduce the drag due to flow separation at the higher lift coefficients. The pitching-moment curve was extended and the stability generally reduced, particularly at the stall; the latter effect probably resulted from the load carried by the slat itself, which effectively extended the wing leading edge forward.

Lateral characteristics.- The static-lateral derivatives of the basic model and all alternate configurations were obtained between sideslip angles of $\pm 5^\circ$ and are presented in figure 5. Results for the wing alone, the wing and fuselage, and the complete basic model (fig. 5(a)) show that the wing alone has a small amount of directional stability as is indicated by the small negative values of C_{n_ψ}, that the wing-fuselage combination is unstable, and that the addition of the vertical fin results in directional stability for the complete V(a'L) configuration.

In figure 5(b) may be observed the effect of wing leading-edge slats on the static stability properties. The linear portions of the curves are extended from $C_L = 0.4$ to $C_L = 0.8$ by means of the slats. It is believed that test results obtained at higher Reynolds numbers would exhibit a similar trend, if the wing surface were kept smooth.

In figure 5(c) is shown the result of moving the vertical fin forward a distance equal to 35 percent of the wing mean aerodynamic chord. It is noted that the values of C_{n_ψ} become less negative even though somewhat larger values of C_{Y_ψ} occur. An investigation into the end-plate effects of fuselages on vertical tails is reported in reference 4 and indicates that the increased values of C_{Y_ψ} for the vertical fin at the forward position is attributable to the increased end-plate effect of the fuselage at that position. The reduction in directional stability results, of course, from the reduction in tail length.

The effects on the static derivatives of varying the lateral position of the vertical fins while maintaining a constant tail length is shown in figures 5(d) and 5(e). It appears that, for comparable fin areas, the $0.43\frac{b}{2}$ fin position is less effective than either the central position or the $0.86\frac{b}{2}$ fin position in producing C_{Y_ψ}, C_{n_ψ}, and C_{l_ψ}. At zero lift, a sizable positive increment in C_{l_ψ} resulted when the fins were moved from the $0.43\frac{b}{2}$ fin position to the $0.86\frac{b}{2}$ fin position. It is believed that the span loading induced on the wing by the vertical fins was responsible for this increment. (See reference 5.) The loading induced on the wing is antisymmetrical and of such a nature that for positive angles of yaw the portions of the wing outboard of the fins produce negative rolling moments and the portions inboard of the fins produce positive rolling moments. With the vertical fins in the $0.43\frac{b}{2}$ position, the induced loadings outboard of the fins are more effective in producing rolling moment than those inboard of the fins which results in a negative increment in C_{l_ψ}. On moving the fins from the $0.43\frac{b}{2}$ position to the $0.86\frac{b}{2}$ position, the portions of the wing outboard of the fins have been decreased and the induced loading outboard of the fins is reduced, resulting in less negative rolling moments, or a positive increment in C_{l_ψ}.

Dorsal fins which extended forward along the wing chord to the leading edge were added to the V(b2L) fins. The results shown in figure 5(f) indicate a small decrement in directional stability due to the forward shift in the effective center of pressure for the fin-dorsal combination. Other investigations (reference 6, for instance) have indicated that the primary effect of a dorsal fin is to increase fin effectiveness only at large yaw angles.

An alternate fin arrangement, V(b4S), wherein the fin area is divided between the upper and lower surfaces of the wing, results in greater fin effectiveness brought about, of course, by the increase in aspect ratio of the fins (fig. 5(f)). A similar increase in effectiveness is evident at the $0.86\frac{b}{2}$ location as is shown in figure 5(g). The V(c4S) arrangement also results in a much more negative value of C_{l_ψ} than does the V(c2L) arrangement. For the divided fin arrangement, a change in lateral position of the fins produced no appreciable change in the fin effectiveness, as is shown in figure 5(h).

Yawing Flow

The yawing stability derivatives presented in figure 6 exhibit properties similar in trend to those for the sideslipping derivatives in figure 5. The fuselage contribution to the damping-in-yaw parameter, C_{n_r}, is negligible at low lift coefficients (fig. 6(a)), and at high lift coefficients, the fuselage decreases the damping in yaw. A decrease in damping in yaw is signified by a less negative value of C_{n_r}. The addition of the vertical fin produced the expected increase in damping and positive increments to C_{l_r} and C_{Y_r}.

The effect on the yawing derivatives of the use of leading-edge wing slats to extend the linear portions of these curves to higher lift coefficients is shown in figure 6(b). It is expected that an increase in the test Reynolds number would, for a smooth wing, produce extensions in the curves somewhat similar to those produced by the slats.

A longitudinal change in position of the vertical fin equal to $0.35\bar{c}$ (fig. 6(c)) produced no sizable change in the yawing characteristics of the model except for a slight decrease in the damping at low lift coefficients for the model with the shorter tail length.

The results for the lateral-fin locations compared in figure 6(d) indicate that the $0.86\frac{b}{2}$ position is the most effective position for vertical fins in producing damping in yaw, although the difference from the results for the other positions is not large. The increase in damping in yaw that appears with movement of the fins away from the plane of symmetry is expected since the difference in drag between the two fins becomes greater as the fins are moved farther from the plane of symmetry. The fin farthest from the center of rotation of the wing, of course, has the higher drag. An investigation into the effects of various outboard and central fins on the yawing derivatives of a triangular-wing model (reference 7) indicated that outboard fins were generally less satisfactory in producing damping in yaw than were central fins - particularly at high angles of attack. The semispan vortices associated with the flow about wings of triangular plan form at high angles of attack appear to subject an outboard fin to induced angles large enough to cause stalling of the fin which is detrimental to the damping in yaw. Since the vortex sweeps inboard with increasing angle of attack, moving the fin inboard will delay the contact of the vortex and the fin to higher angles of attack. For the more conservative wing tested in the present investigation, the flow disturbances in the region of the fins on the wing are less severe than those for the triangular wing and the effectiveness of the outboard fins is maintained.

For the larger fin area, and for the fin area entirely on the upper surface of the wing, the outboard location V(c2L) is more effective than the inboard location V(b2L) in producing the derivatives C_{Y_r}, C_{n_r}, and C_{l_r} (fig. 6(e)). The addition of dorsal fins to V(b2L) resulted in no appreciable change in the damping in yaw (fig. 6(f)). At the $0.86\frac{b}{2}$ position, the V(c2L) arrangement is slightly more favorable than the V(c4S) arrangement for producing damping in yaw (fig. 6(g)).

The tests made with the V(b4S) arrangement in the yawing condition yielded results which were unreasonable and which were not consistent with the results of subsequent check tests. The lack of consistency in yawing-flow data for this fin arrangement is probably due to the close proximity of the lower fins to the support strut. Because of the doubtful nature of these data, results for the V(b4S) arrangement are not presented for the yawing condition.

The relative effectiveness of vertical fins changes considerably with changes in fin location and area and with changes in model angle of attack. It is apparent that no single fin arrangement is superior to all others in all the aerodynamic qualities considered in vertical-fin design. In generalizing, however, it appears that, for comparable fin areas and equal tail lengths, fins located at the 86-percent spanwise location are more satisfactory for providing directional stability and damping in yaw than fins placed at the 43-percent spanwise location. The central fin has more directional stability, but less damping at low lift coefficients, than the twin fins located at either outboard position. The central fin has the advantage over the outboard fins in that the directional stability and damping tended to increase slightly at high lift coefficients. With the fins at the outboard locations, the trend is for the effectiveness to decrease in the high-lift-coefficient region.

Rolling Flow

Changes in vertical-fin arrangement had no great effect on the damping-in-roll parameter C_{l_p} but, in some cases, resulted in significant changes in the lateral force due to rolling C_{Y_p} and the yawing moment due to rolling C_{n_p} (fig. 7).

The effect of the addition of the slat, shown in figure 7(b), is again the extension of the linear portions of the curves to higher lift coefficients than occurred without the slat. Movement of the vertical fin to the forward central location increased the damping in roll by about 10 percent (fig. 7(c)) apparently because of the increased end-plate

effect of the fuselage. For either the small fins or the large fins (fig. 7(d) and (e), respectively), it appears that in moving from the $0.43\frac{b}{2}$ to the $0.86\frac{b}{2}$ spanwise location a sizable decrement occurs in C_{Y_p} with a resulting increment in C_{n_p} in the lower-lift-coefficient range where such changes in C_{n_p} have been shown to be particularly important in dynamic stability analysis. The changes are somewhat greater for the large fins than they are for the small fins. The increase in C_{n_p} that occurred in changing from the V(b2S) to the V(c2S) arrangement and from the V(b2L) to the V(c2L) arrangement did not again materialize in changing from the V(b4S) to the V(c4S) arrangement (fig. 7(g)) since in the divided-fin configuration the yawing moments due to fins on opposite wing surfaces oppose each other.

COMPARISON WITH CALCULATED RESULTS

A comparison is made in figure 8 of the experimental derivatives and those calculated by currently available methods for the wing alone (references 8, 9, 10, and 11). Since the static derivatives can be determined rather simply in conventional wind tunnels, emphasis has been placed on the development of calculation methods for the rotary derivatives by both theoretical and empirical means.

In figure 8, it is shown that the calculation methods serve as reasonably good estimation procedures at least at low lift coefficients. As is pointed out in reference 10, the variation of most derivatives with lift coefficient departs from linearity at relatively low lift coefficients. The departure point may be predicted by noting the lift coefficient at which the quantity $C_D - \frac{C_L^2}{\pi A}$ begins a rapid rise. This point occurred at $C_L = 0.3$ for the wing tested. The rise in $C_D - \frac{C_L^2}{\pi A}$ is associated with partial separation which is delayed for smooth wings by higher Reynolds numbers. The effect of the higher Reynolds numbers, then, would be to extend the linear portions of these stability parameter curves to higher lift coefficients. For a full-scale airplane, the actual derivatives at high lift coefficients could conceivably lie anywhere between the two extremes of the low-speed experimental and the extrapolated curves.

The increments in the derivatives which are due to the vertical fin alone in the V(a'L) arrangement are shown in figure 9. Since no attempt has been made herein to analyze wing or fuselage interference effects, these effects are included in the vertical-fin contributions shown. The most logical explanation for changes in vertical-fin effectiveness for various fin locations and arrangements is a variation in end-plate effect of the fuselage or the wing on the fin. A comprehensive investigation has been made and is reported in reference 4 on the effective aspect ratio of a vertical fin in the presence of a fuselage. It is shown that fin effectiveness is a function of the fuselage diameter at the vertical tail. From this study an effective aspect ratio of 2.54 was determined for the vertical tail as compared with the geometric aspect ratio of 1.85. The calculations shown in figure 9 were made using lift-curve slopes from reference 3 and simple geometric considerations such as those of reference 12. In addition, a correction from reference 13 was used in calculating the rolling derivatives to account for wing interference at least partially.

Reference 14 presents the results of an investigation into the effectiveness of vertical tails in the presence of horizontal tails. Because it is shown that the span of the horizontal tail is of little importance in its effect on the vertical tail, it is believed that these results are applicable to wing-mounted fins. In figure 10, the variations of the fin increments in the derivatives due to changes in lateral location are shown for all fin arrangements. These increments are compared with values calculated as they were for the values shown in figure 9. An aspect-ratio correction of 1.4 determined from reference 14 was used for the fins mounted on the wing. These wing-mounted fins are assumed to be free of any effects of sidewash due to the unsymmetrical span loading of the wing in roll. The corrections of reference 13 were applied to the rolling derivatives for the centrally located fins, however.

In most cases the magnitude of the vertical-fin increments to the stability derivatives can be estimated with reasonable accuracy. Where sizable differences appeared between the estimated and the experimental results, these differences must be attributed to inadequacies in the theory. A more rigorous theory would permit more accurate estimation of those effects which heretofore have been considered approximately, such as the change in end-plate effect of the wing on the vertical fin at various spanwise and chordwise locations of the fin. The more rigorous theory would also include the profile and induced drag of the fins and the effects on the fins of mutual wing-fuselage interference and of sidewash from the fuselage.

CONCLUSIONS

The following conclusions have been drawn from an investigation into the effects of vertical-fin location and area on the stability derivatives of a semitailless airplane model of representative configuration:

1. The contributions of the vertical fin to the stability derivatives generally could be estimated with reasonable accuracy by simple considerations, wherein interference effects approximately were accounted for, in spite of the unusually short tail length and large tail height of this configuration.

2. For comparable fin areas and equal tail lengths, fins located at the 86-percent spanwise location are, in general, more satisfactory for providing directional stability and damping in yaw than fins placed at the 43-percent spanwise location, although the differences in effectiveness in most cases are not large. In the low-lift-coefficient region, a single central fin provided more directional stability but less damping in yaw than twin fins located at either outboard position. The central fin has an advantage over the outboard fins in that the fin effectiveness tends to increase slightly at high lift coefficients, while the trend is for the outboard fins to suffer a decrease in effectiveness in this lift-coefficient region.

3. Changes in vertical-fin arrangement had no appreciable effect on the damping in roll but, in some cases, resulted in significant changes in the yawing moment due to rolling.

4. Vertical fins located at the 43-percent spanwise position on the upper wing surface contributed a negative increment to the effective dihedral parameter; at the 86-percent spanwise position, they contributed a sizable positive increment. This change in sign of the effective dihedral with lateral movement of the fins is believed to be the result of the nature of the span loadings induced on the wing by the lift on the fins.

Langley Aeronautical Laboratory
National Advisory Committee For Aeronautics
Langley Field, Va.

REFERENCES

1. Bird, John D., Jaquet, Byron M., and Cowan, John W.: Effect of Fuselage and Tail Surfaces on Low-Speed Yawing Characteristics of a Swept-Wing Model as Determined in Curved-Flow Test Section of Langley Stability Tunnel. NACA RM L8G13, 1948.

2. MacLachlan, Robert, and Letko, William: Correlation of Two Experimental Methods of Determining the Rolling Characteristics of Unswept Wings. NACA TN 1309, 1947.

3. DeYoung, John: Theoretical Additional Span Loading Characteristics of Wings with Arbitrary Sweep, Aspect Ratio, and Taper Ratio. NACA TN 1491, 1947.

4. Queijo, M. J., and Wolhart, Walter D.: Experimental Investigation of the Effect of Vertical-Tail Size and Length and of Fuselage Shape and Length on the Static Lateral Stability Characteristics of a Model with 45° Sweptback Wing and Tail Surfaces. NACA TN 2168, 1950.

5. Katzoff, S., and Mutterperl, William: The End-Plate Effect of a Horizontal-Tail Surface on a Vertical Tail Surface. NACA TN 797, 1941.

6. Thompson, F. L., and Gilruth, R. R.: Notes on the Stalling of Vertical-Tail Surfaces and on Fin Design. NACA TN 778, 1940.

7. Goodman, Alex: Effect of Various Outboard and Central Fins on Low-Speed Yawing Stability Derivatives of a 60° Delta-Wing Model. NACA RM L50E12a, 1950.

8. Toll, Thomas A., and Queijo, M. J.: Approximate Relations and Charts for Low-Speed Stability Derivatives of Swept Wings. NACA TN 1581, 1948.

9. Campbell, John P., and Goodman, Alex: A Semiempirical Method for Estimating the Rolling Moment Due to Yawing of Airplanes. NACA TN 1984, 1949.

10. Goodman, Alex, and Fisher, Lewis R.: Investigation at Low Speeds of the Effect of Aspect Ratio and Sweep on Rolling Stability Derivatives of Untapered Wings. NACA Rep. 968, 1950.

11. Goodman, Alex, and Adair, Glenn H.: Estimation of the Damping in Roll of Wings Through the Normal Flight Range of Lift Coefficient. NACA TN 1924, 1949.

12. Bamber, Millard J.: Effect of Some Present-Day Airplane Design Trends on Requirements for Lateral Stability. NACA TN 814, 1941.

13. Letko, William, and Riley, Donald R.: Effect of an Unswept Wing on the Contribution of Unswept-Tail Configurations to the Low-Speed Static- and Rolling-Stability Derivatives of a Midwing Airplane Model. NACA TN 2175, 1950.

14. Murray, Harry E.: Wind-Tunnel Investigation of End-Plate Effects of Horizontal Tails on a Vertical Tail Compared with Available Theory. NACA TN 1050, 1946.

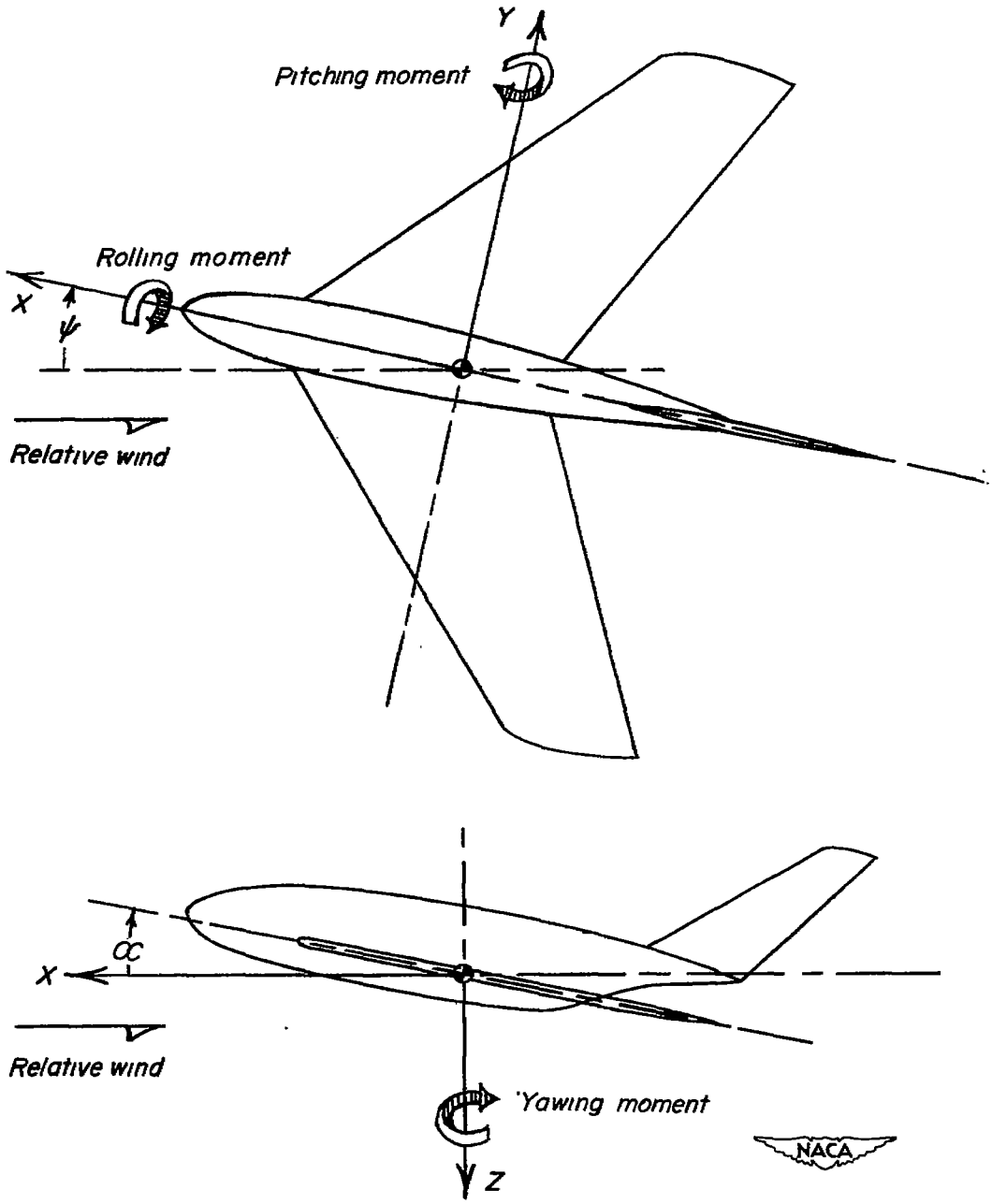

Figure 1.- The stability system of axes. Arrows indicate positive directions of forces, moments, and angular displacements. This system of axes is defined as an orthogonal system having the origin at the center of gravity and in which the Z-axis is in the plane of symmetry and perpendicular to the relative wind, the X-axis is in the plane of symmetry and perpendicular to the Z-axis, and the Y-axis is perpendicular to the plane of symmetry.

	Wing	Fin L	Fin S
Aspect ratio	3.60	1.85	1.85
Taper ratio	0.455	0.444	0.444
Area, sq ft	3.13	0.30	0.15
Span, ft	3.36	0.75	0.53
Sweep, L. E., deg	41.57°	41.54°	41.54°
Mean aerodynamic chord, ft	0.976	0.420	0.296
Airfoil section	NACA 0010-64		

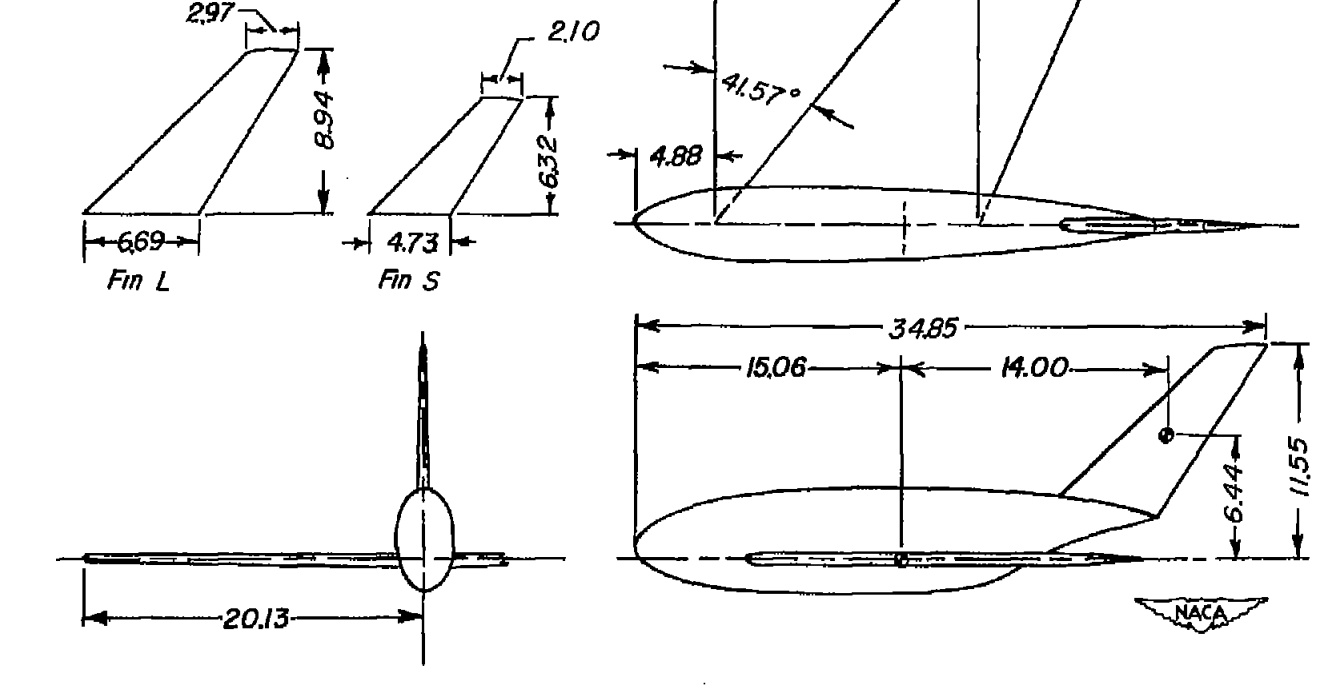

(a) Basic configuration; vertical-fin arrangement V(a'L).

Figure 2.- Description of semitailless model. All dimensions are in inches.

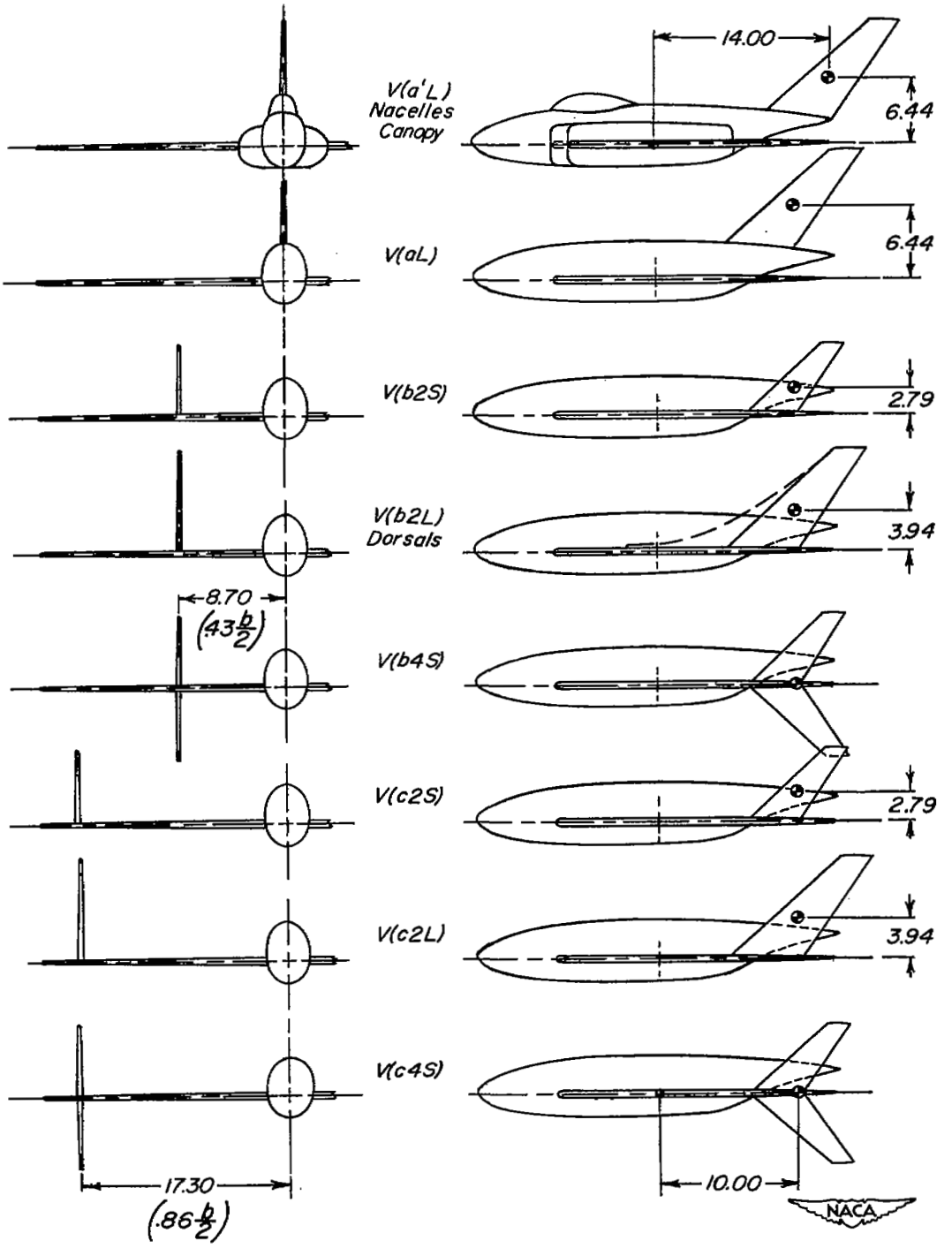

(b) Additional fin arrangements tested.

Figure 2.- Continued.

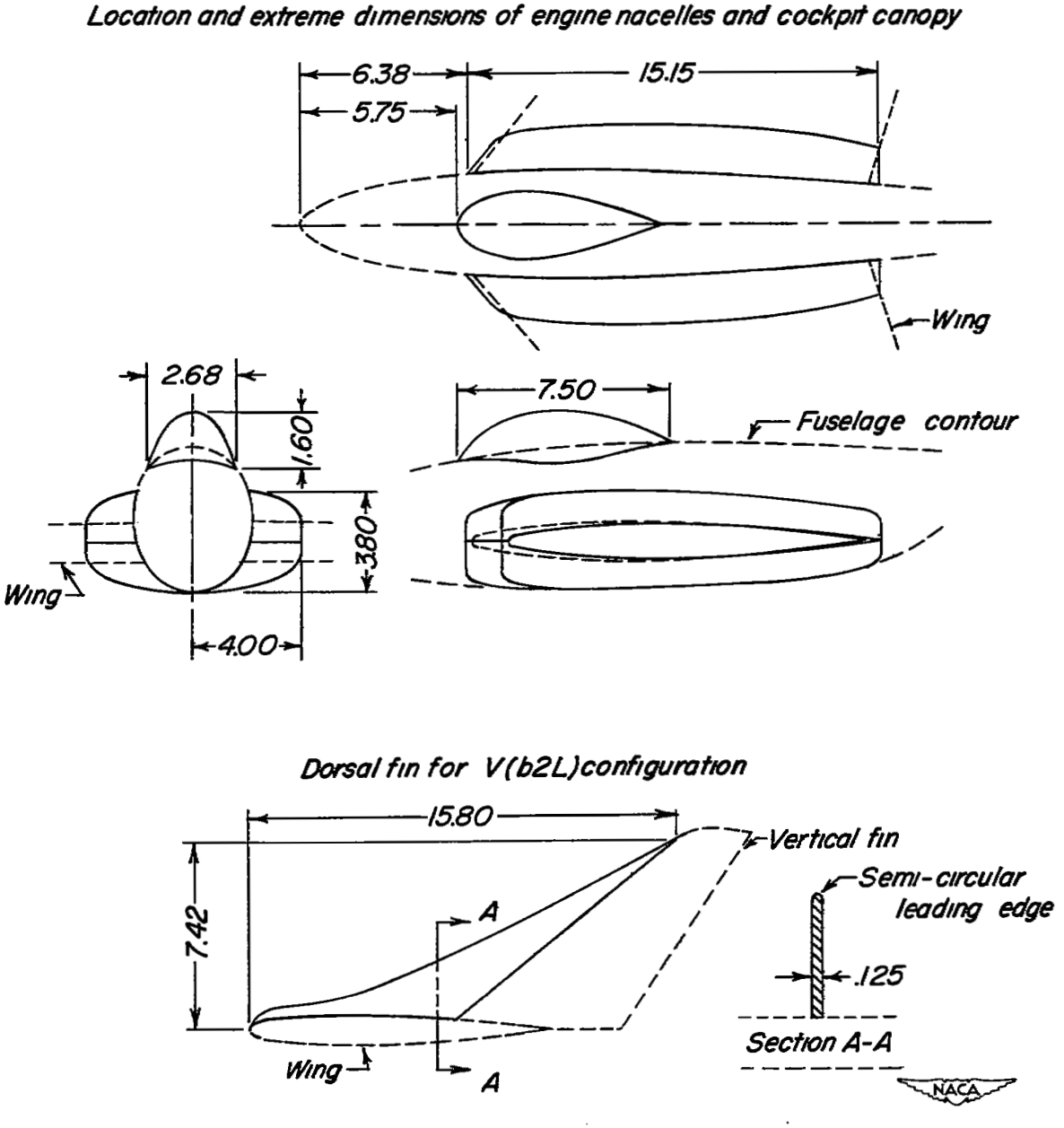

(c) Details of cockpit canopy, engine nacelles, and dorsal fins.

Figure 2.- Concluded.

(a) Vertical-fin configuration V(a'L).

(b) Vertical-fin configuration V(b2L).

(c) Vertical-fin configuration V(b4S).

NACA L-68421

Figure 3.- Semitailless airplane model mounted in the curved-flow test section of the Langley stability tunnel.

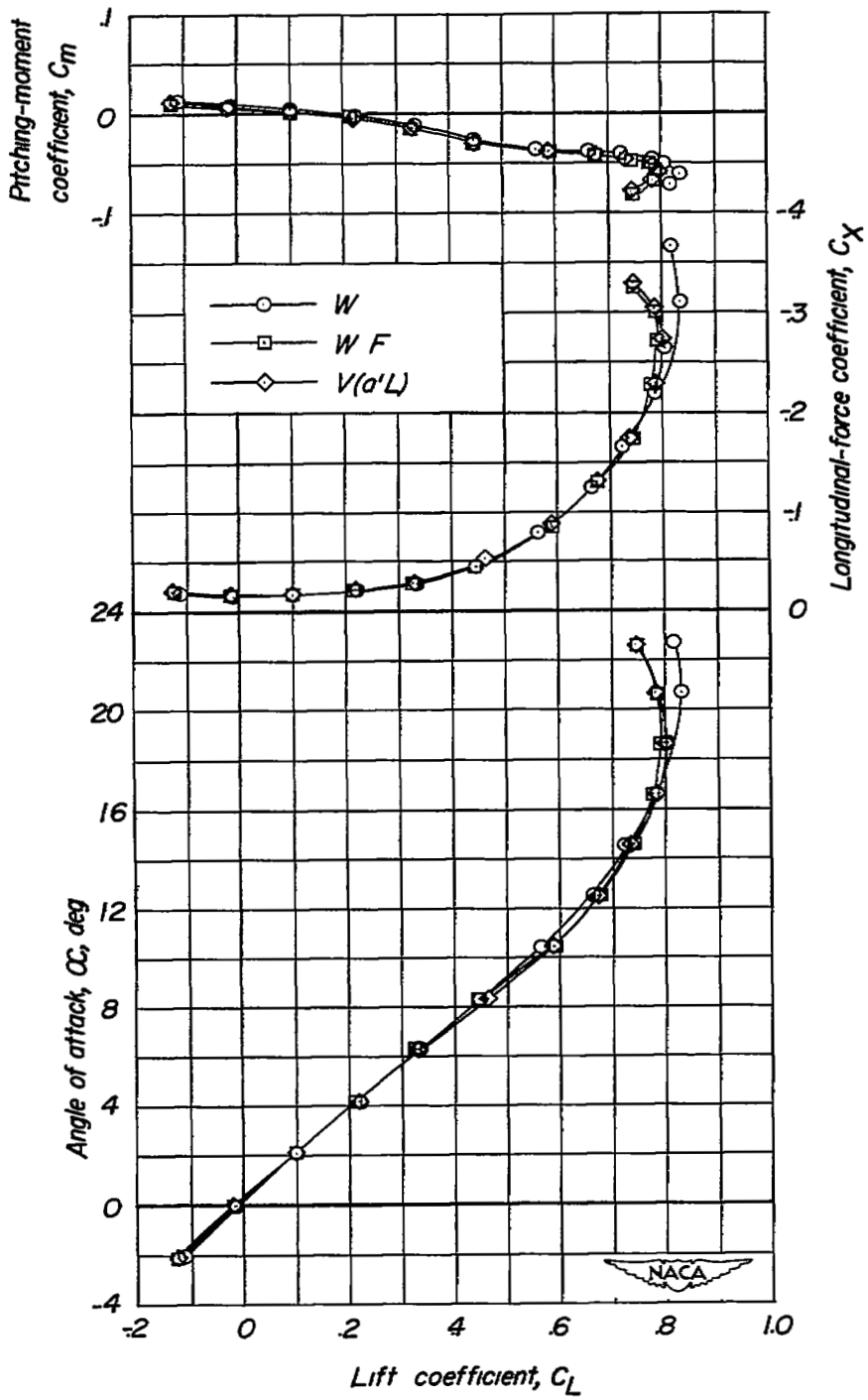

(a) Component parts of basic model.

Figure 4.- Aerodynamic characteristics of semitailless airplane model.

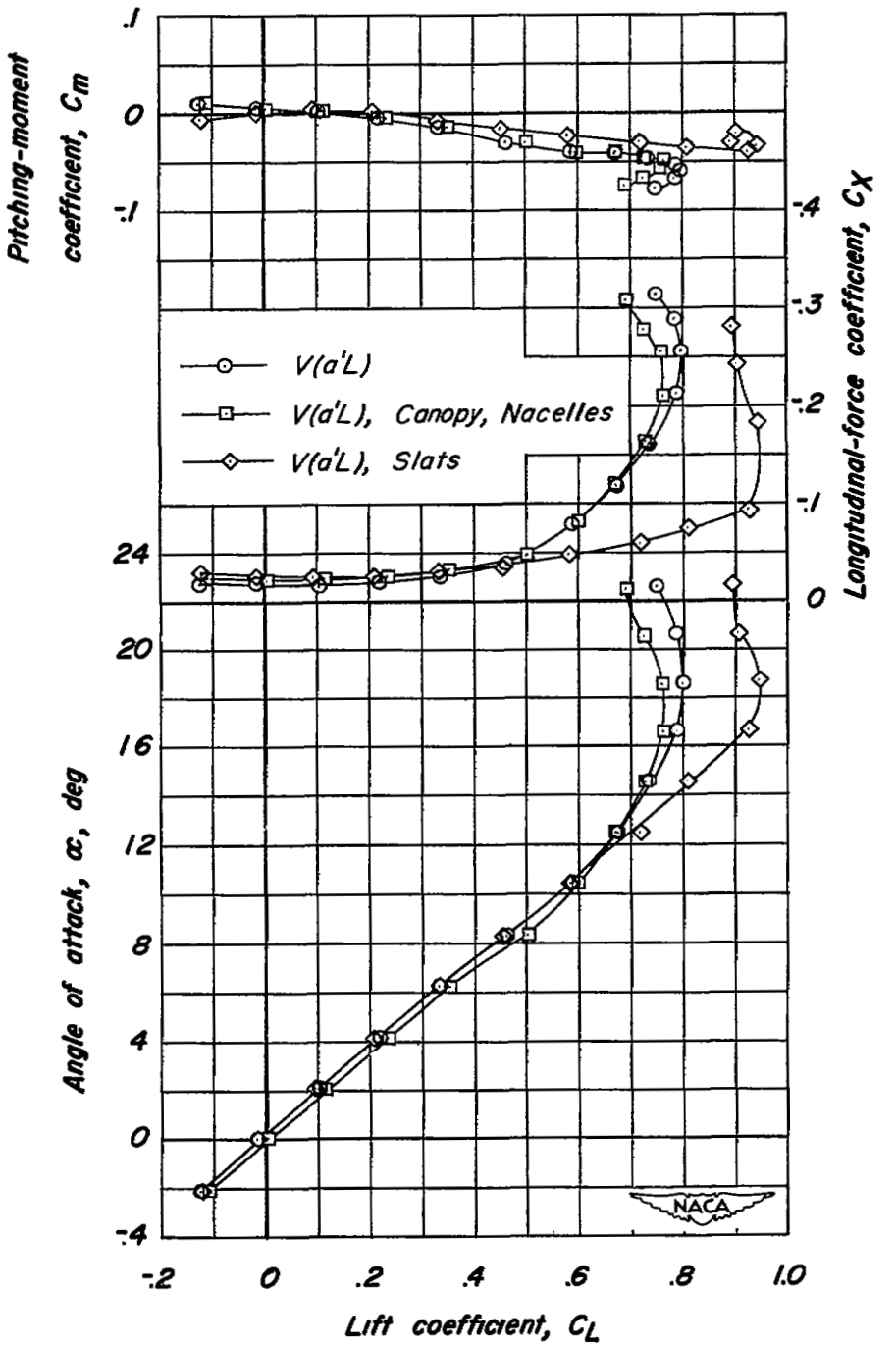

(b) Effects of canopy, nacelles, and slats..

Figure 4.- Concluded.

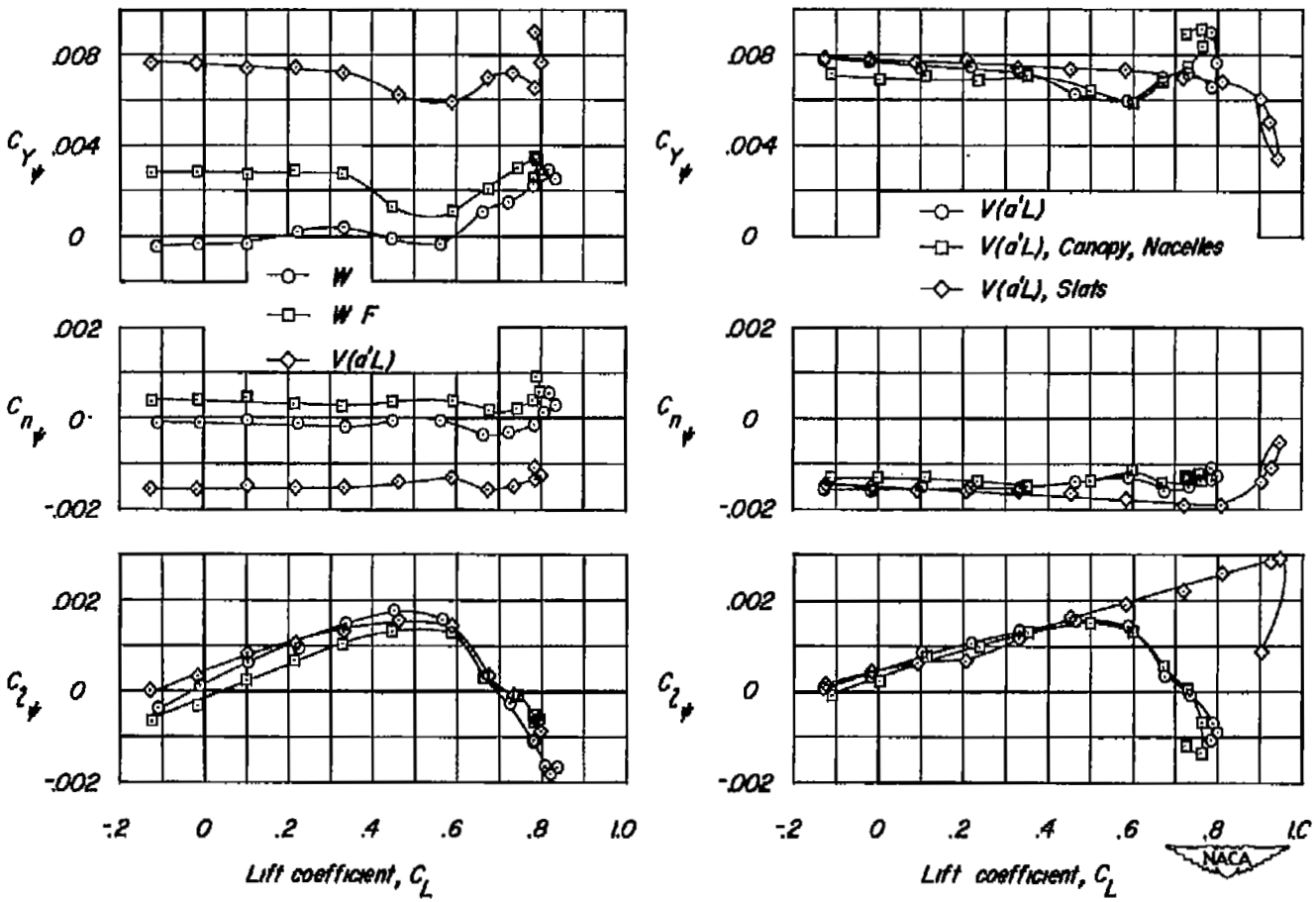

(a) Effect of component parts of basic configuration.

(b) Effect of cockpit canopy, wing-root nacelles, and leading-edge slats as additions to basic configuration.

Figure 5.- The variation with lift coefficient of the static lateral stability derivatives for a semitailless airplane model.

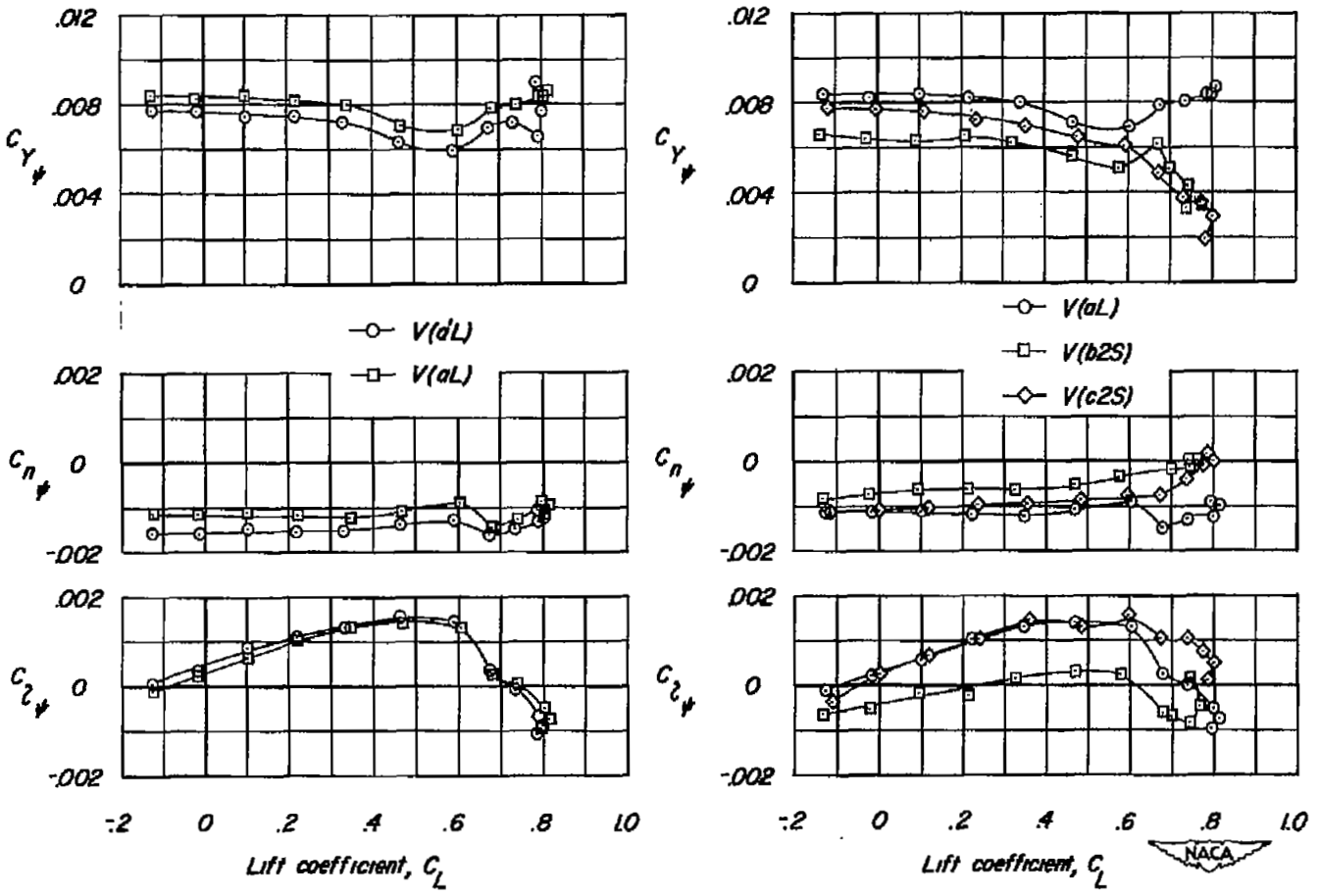

(c) Effect of longitudinal position of vertical fin. $\frac{l_t}{\bar{c}}$ = 1.20, 0.85.

(d) Effect of lateral position of vertical fins for constant fin area and tail length. $\frac{y}{b/2}$ = 0, 0.43, 0.86.

Figure 5.- Continued.

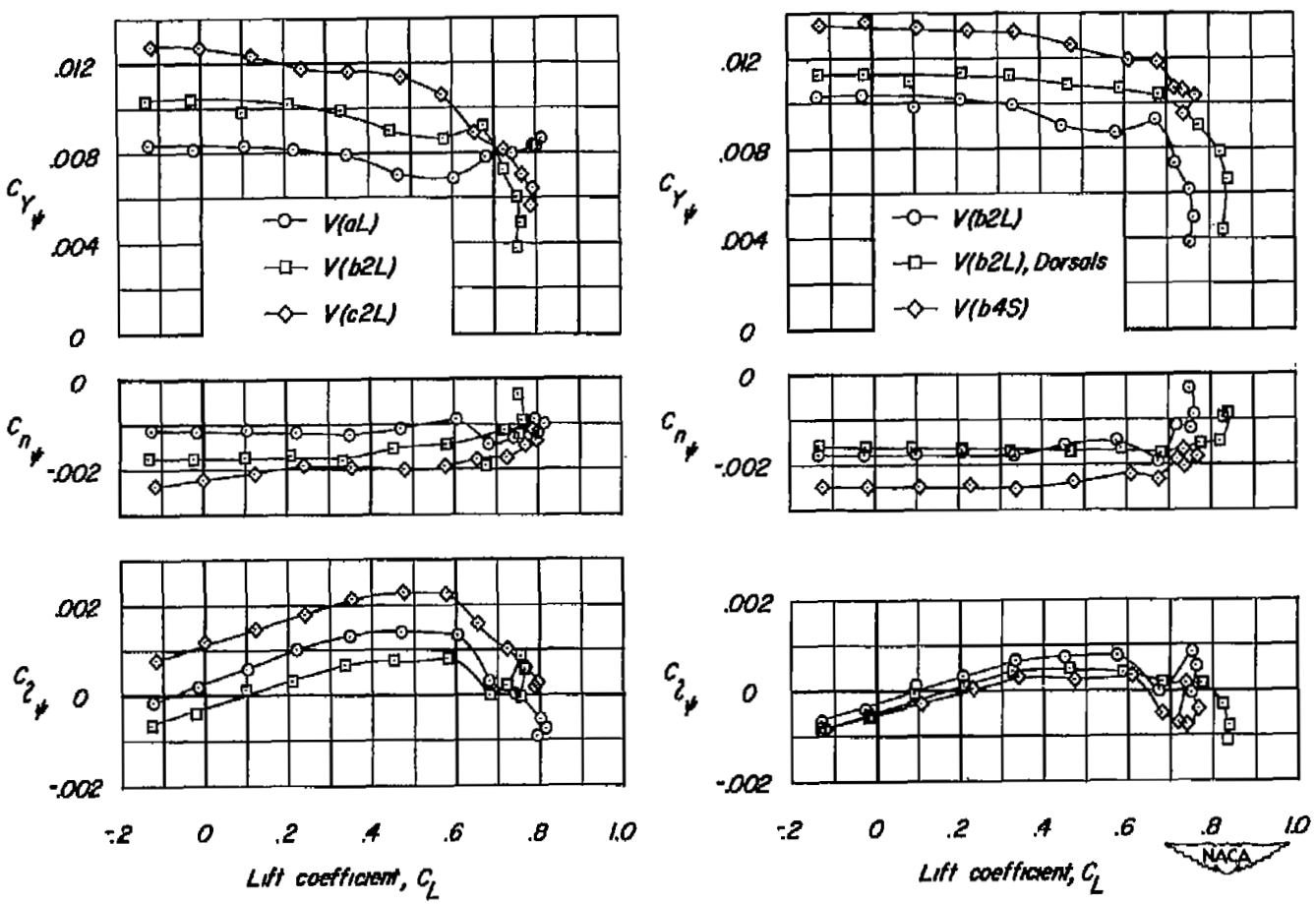

(e) Effect of lateral position and increased area for vertical fins with same tail length. $\frac{y}{b/2} = 0$, 0.43, 0.86.

(f) Effect of dorsal addition to inboard wing fin and alternate arrangement of fin area. $\frac{y}{b/2} = 0.43$.

Figure 5.- Continued.

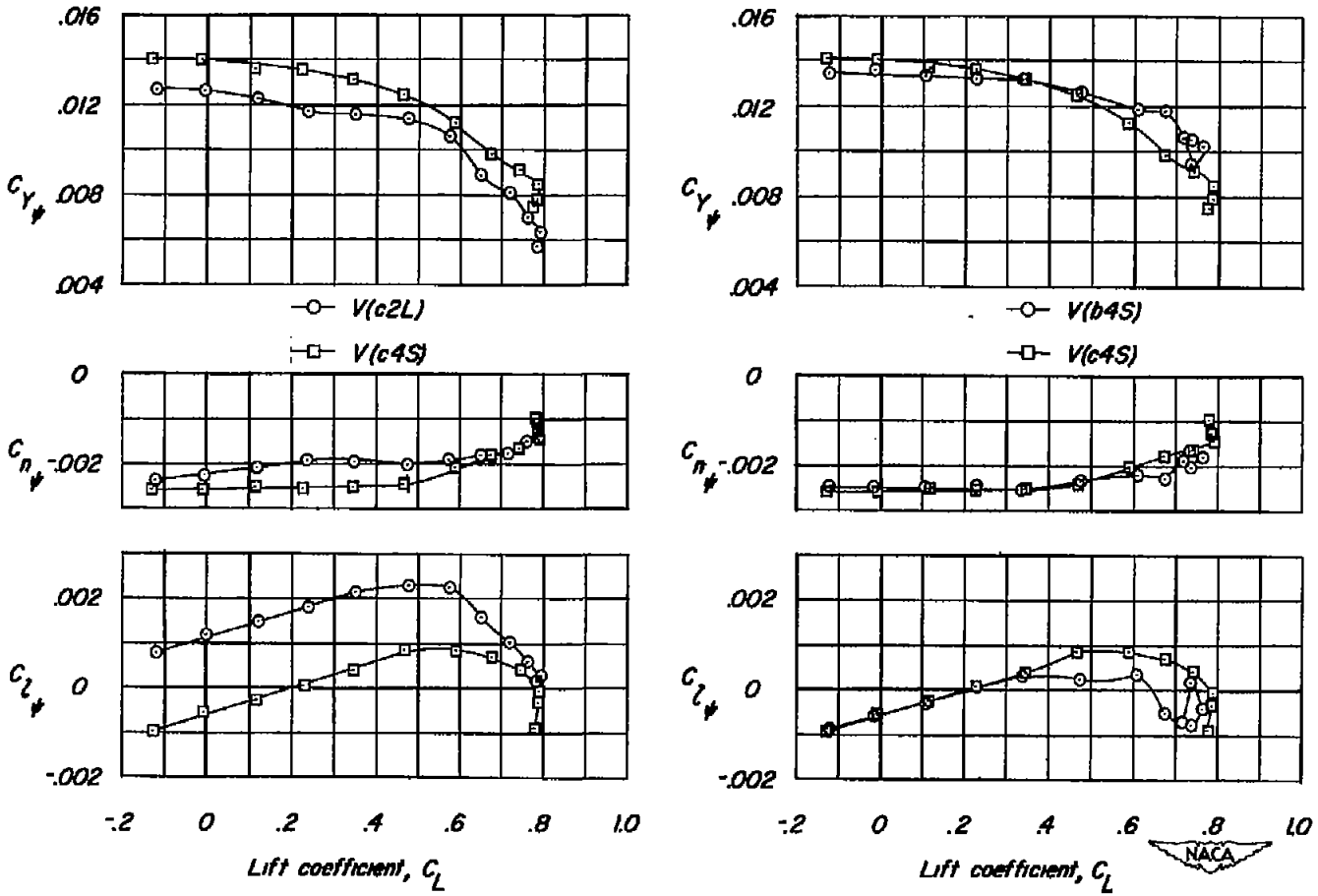

(g) Effect of alternate arrangement of fin area at outboard wing position. $\frac{y}{b/2} = 0.86$.

(h) Effect of lateral position for the alternate fin arrangement. $\frac{y}{b/2} = 0.43, 0.86$.

Figure 5.- Concluded.

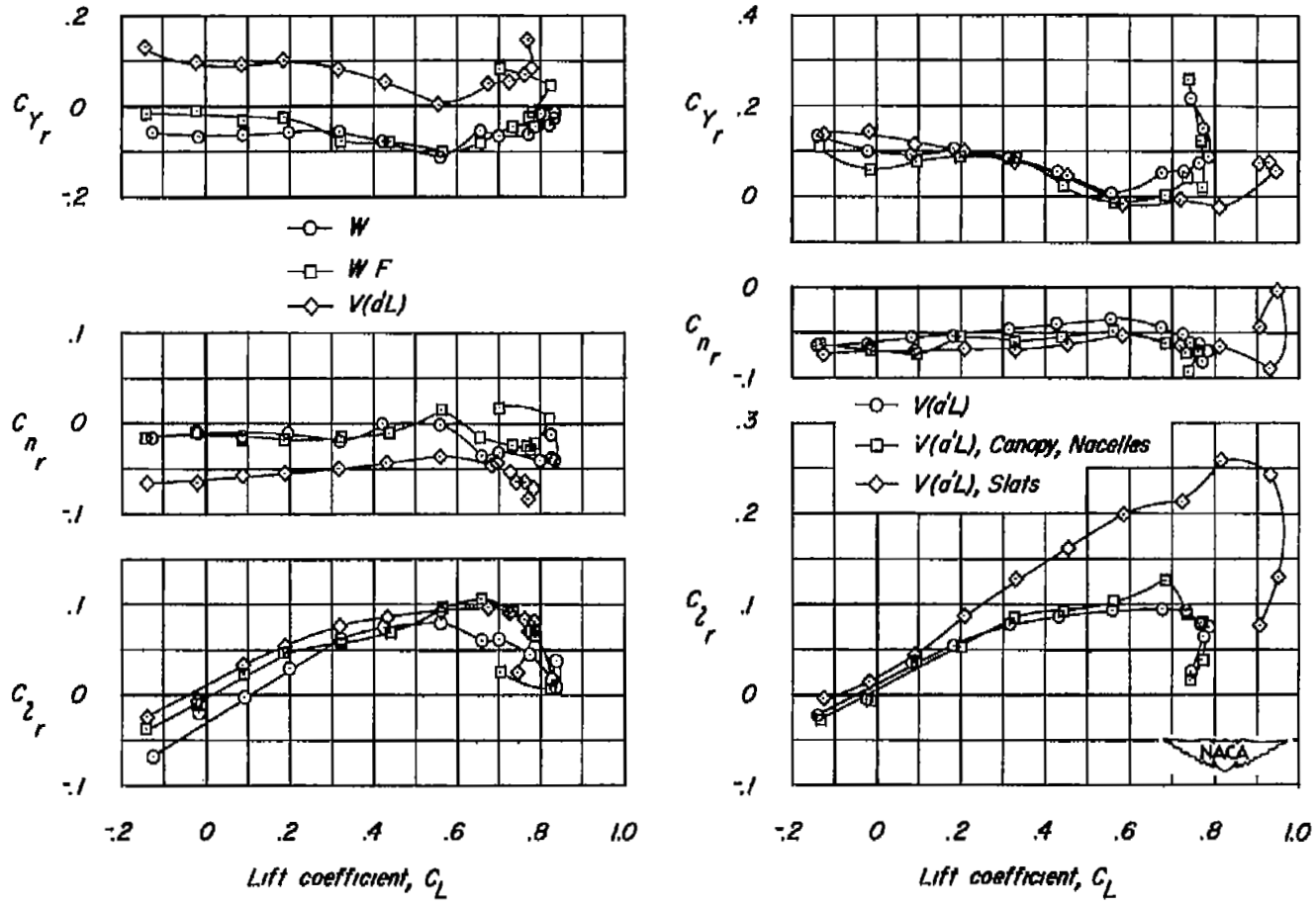

(a) Effect of component parts of basic configuration.

(b) Effect of cockpit canopy, wing-root nacelles, and leading-edge slats as additions to basic configuration.

Figure 6.- The variation with lift coefficient of the yawing stability derivatives for a semitailless airplane model.

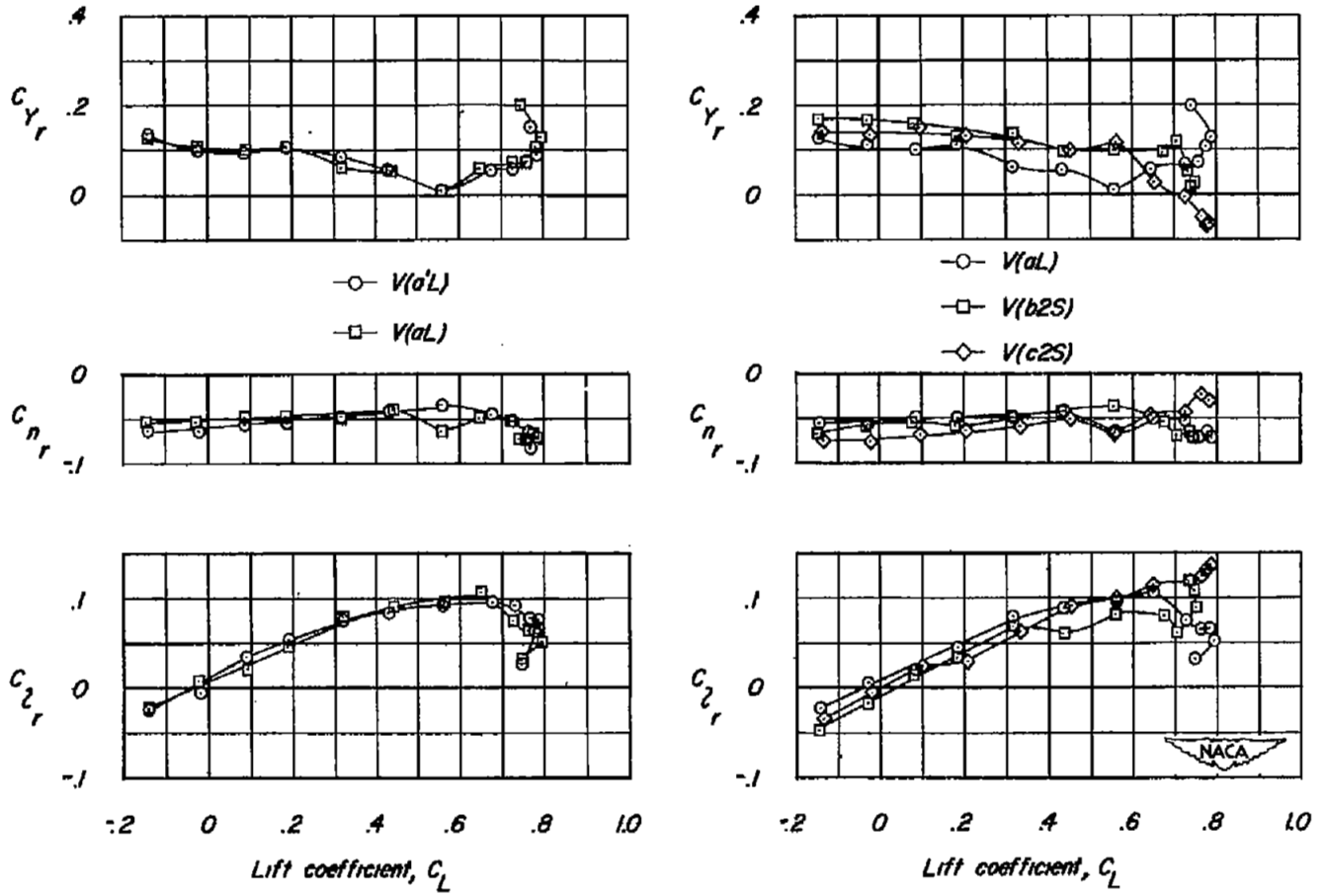

(c) Effect of longitudinal position of vertical fin. $\frac{l_t}{c}$ = 1.20, 0.85.

(d) Effect of lateral position of vertical fins for constant fin area and tail length. $\frac{y}{b/2}$ = 0, 0.43, 0.86.

Figure 6.- Continued.

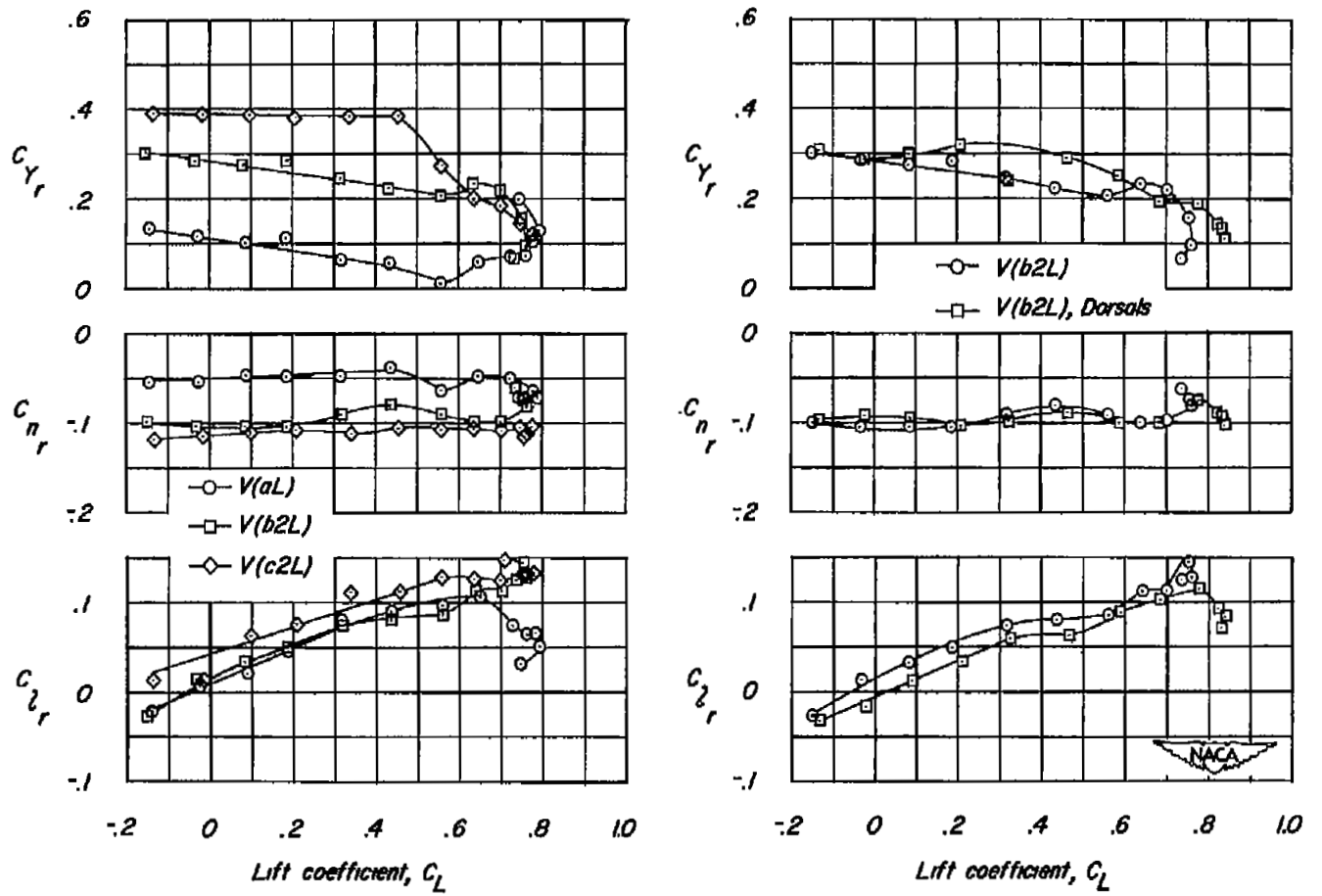

(e) Effect of lateral position and increased area for vertical fins with same tail length. $\frac{y}{b/2}$ = 0, 0.43, 0.86.

(f) Effect of dorsal addition to inboard wing fin. $\frac{y}{b/2}$ = 0.43.

Figure 6.- Continued.

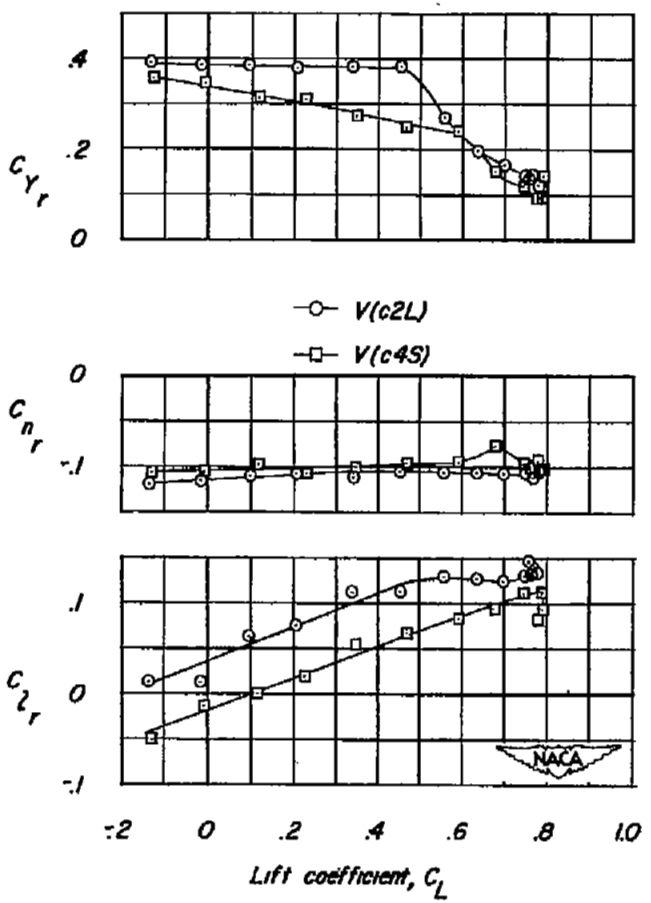

(g) Effect of alternate arrangement of fin area at outboard wing position. $\frac{y}{b/2} = 0.86$.

Figure 6.- Concluded.

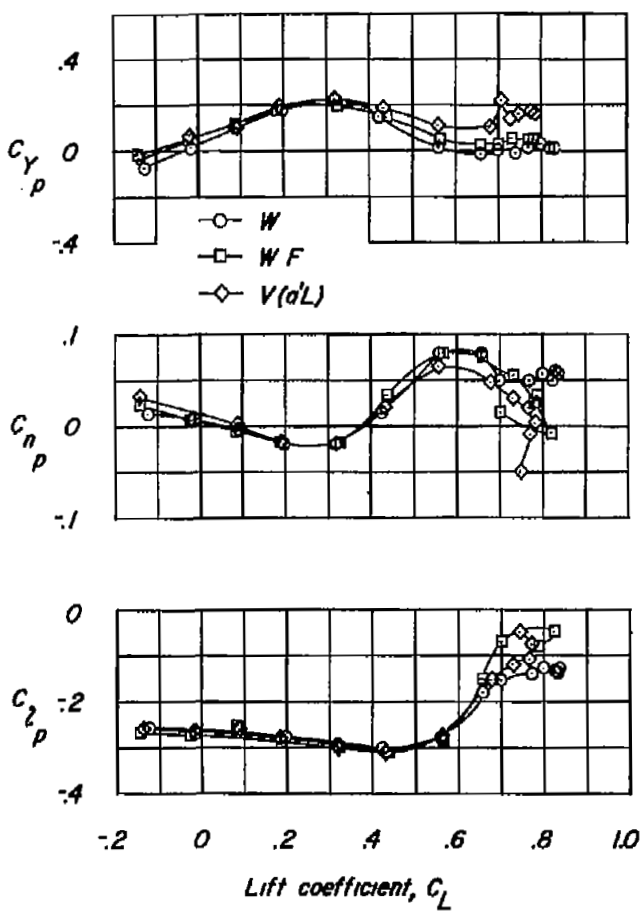

(a) Effect of component parts of basic configuration.

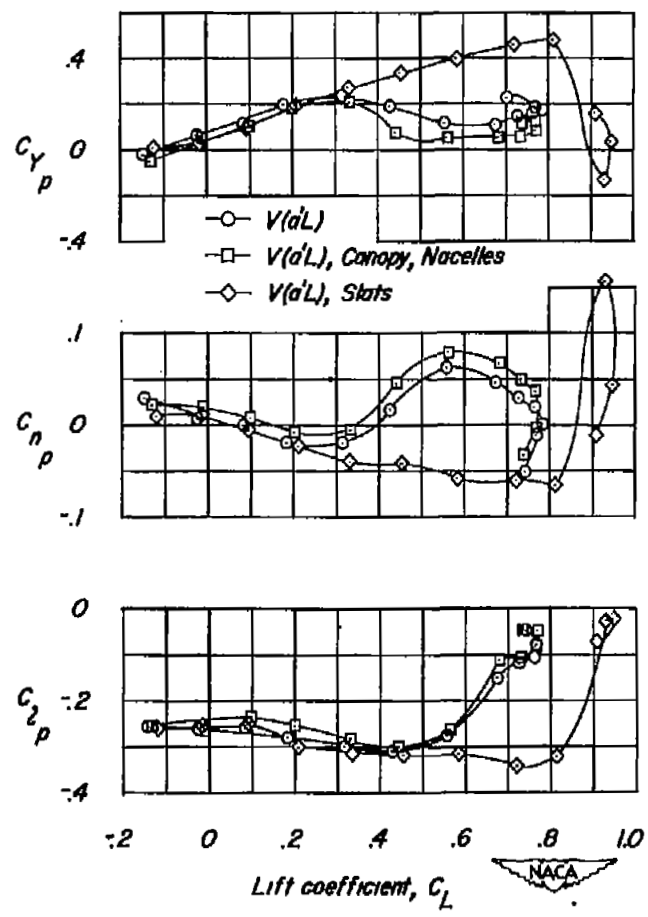

(b) Effect of cockpit canopy, wing-root nacelles, and leading-edge slats as additions to basic configuration.

Figure 7.- The variation with lift coefficient of the rolling stability derivatives for a semitailless airplane model.

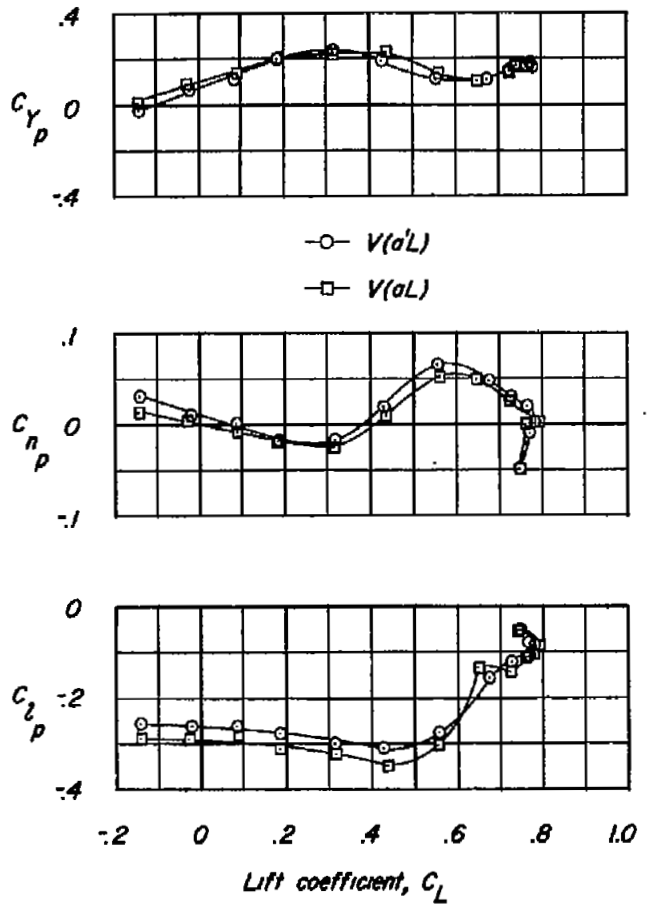

(c) Effect of longitudinal position of vertical fin. $\frac{l_t}{c} = 1.20$, 0.85.

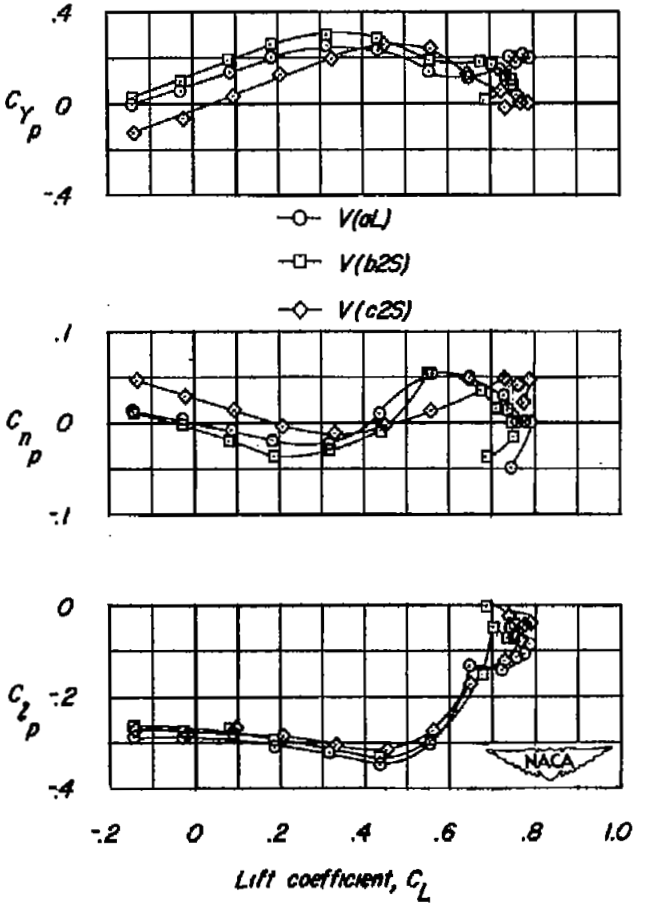

(d) Effect of lateral position of vertical fins for constant fin area and tail length. $\frac{y}{b/2} = 0$, 0.43, 0.86.

Figure 7.- Continued.

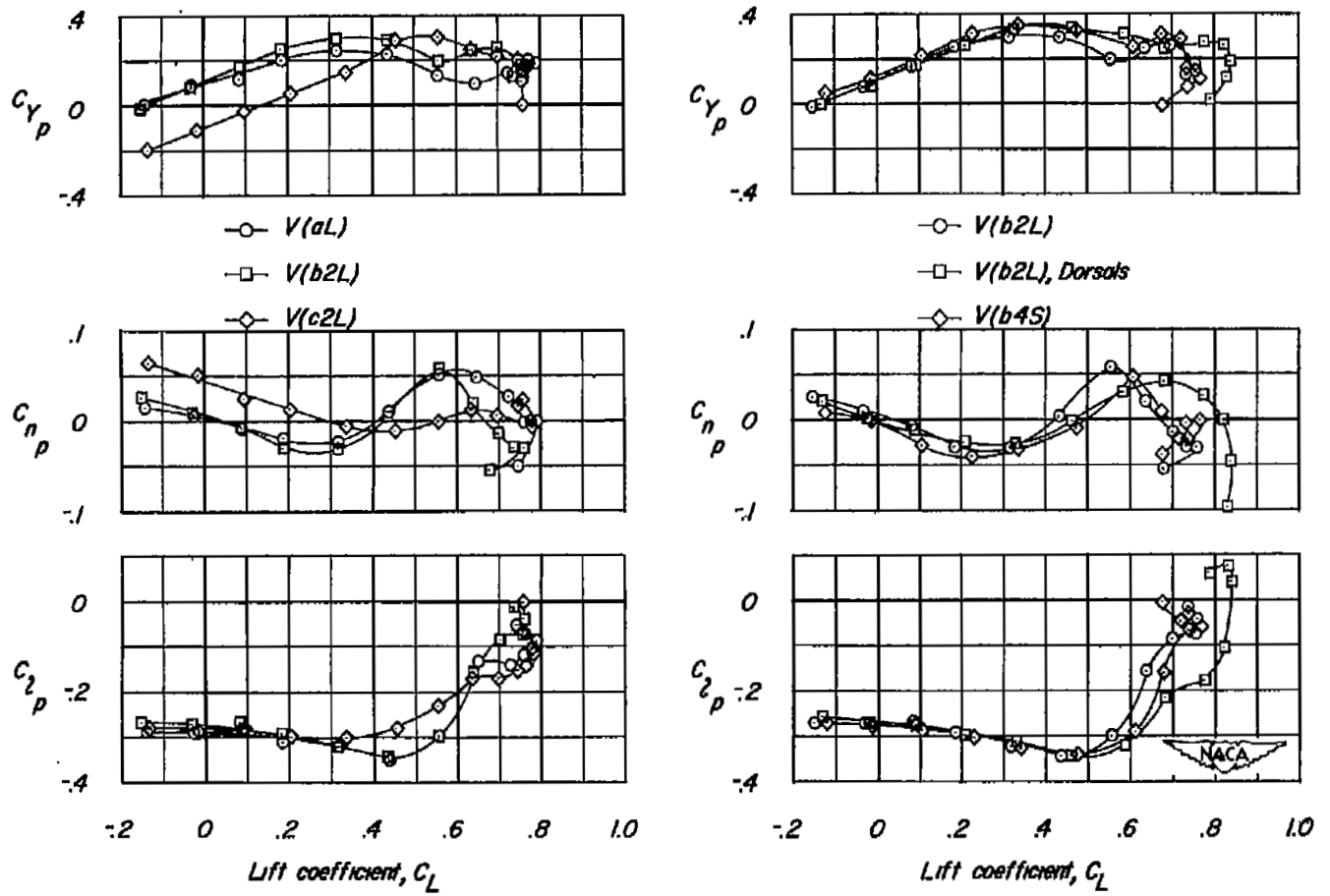

(e) Effect of lateral position and increased area for vertical fins with same tail length. $\frac{y}{b/2} = 0$, 0.43, 0.86.

(f) Effect of dorsal addition to inboard wing fin and alternate arrangement of fin area. $\frac{y}{b/2} = 0.43$.

Figure 7.- Continued.

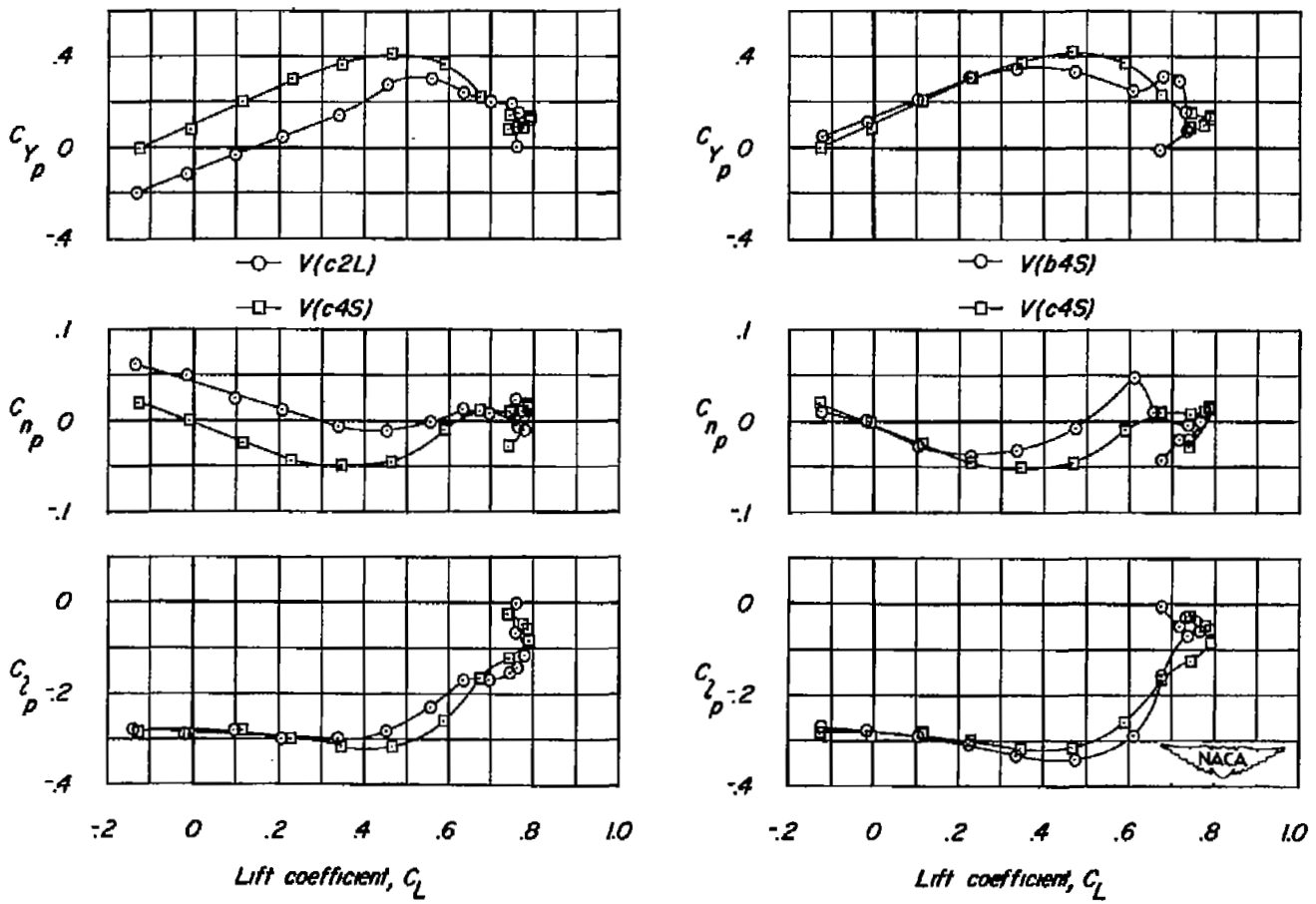

(g) Effect of alternate arrangement of fin area at outboard wing position. $\frac{y}{b/2} = 0.86$.

(h) Effect of lateral position for the alternate fin arrangement. $\frac{y}{b/2} = 0.43, 0.86$.

Figure 7.- Concluded.

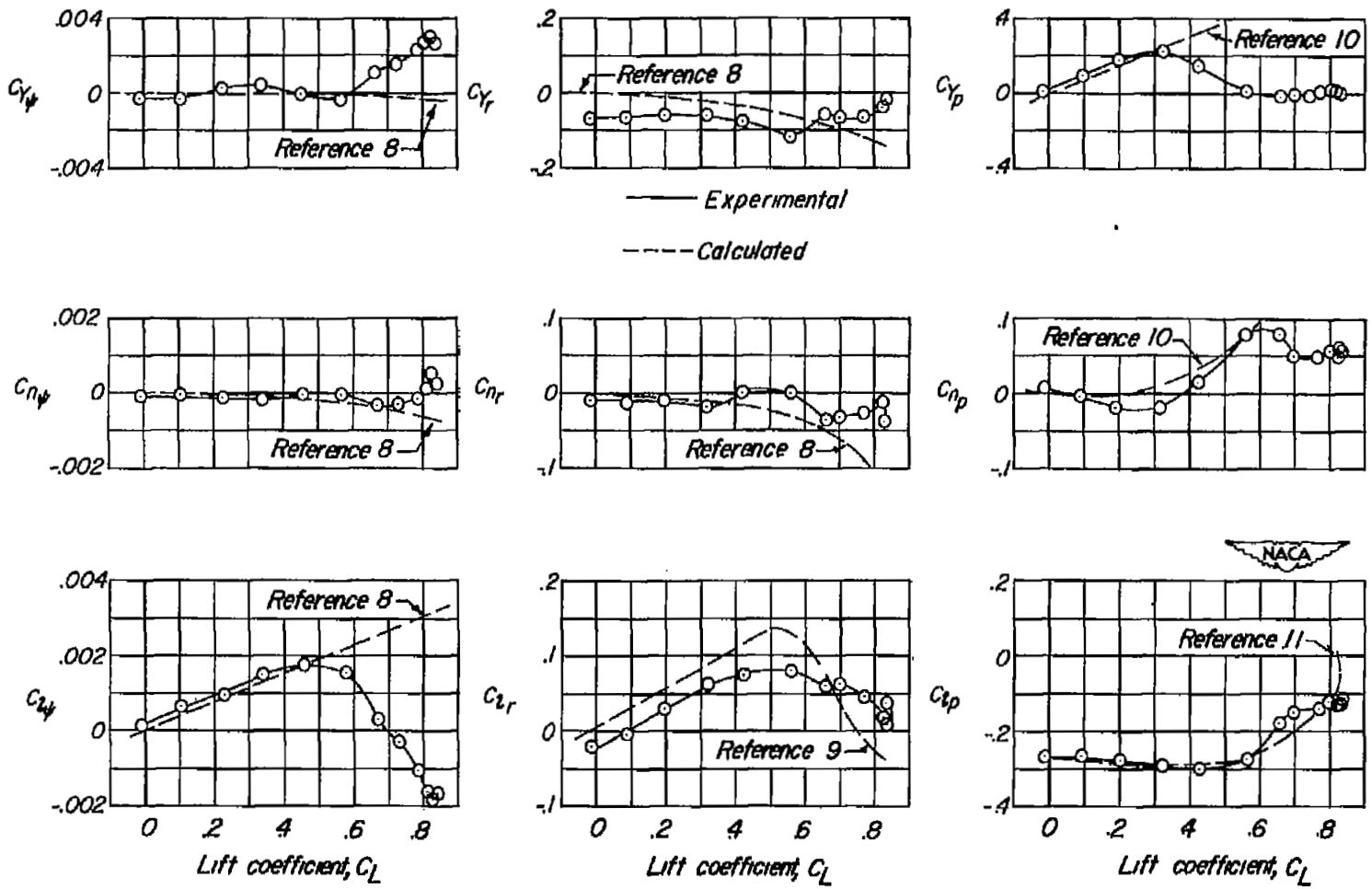

Figure 8.- The variation with lift coefficient of the stability derivatives for the wing alone. A = 3.60, λ = 0.455, Λ_{LE} = 41.57°.

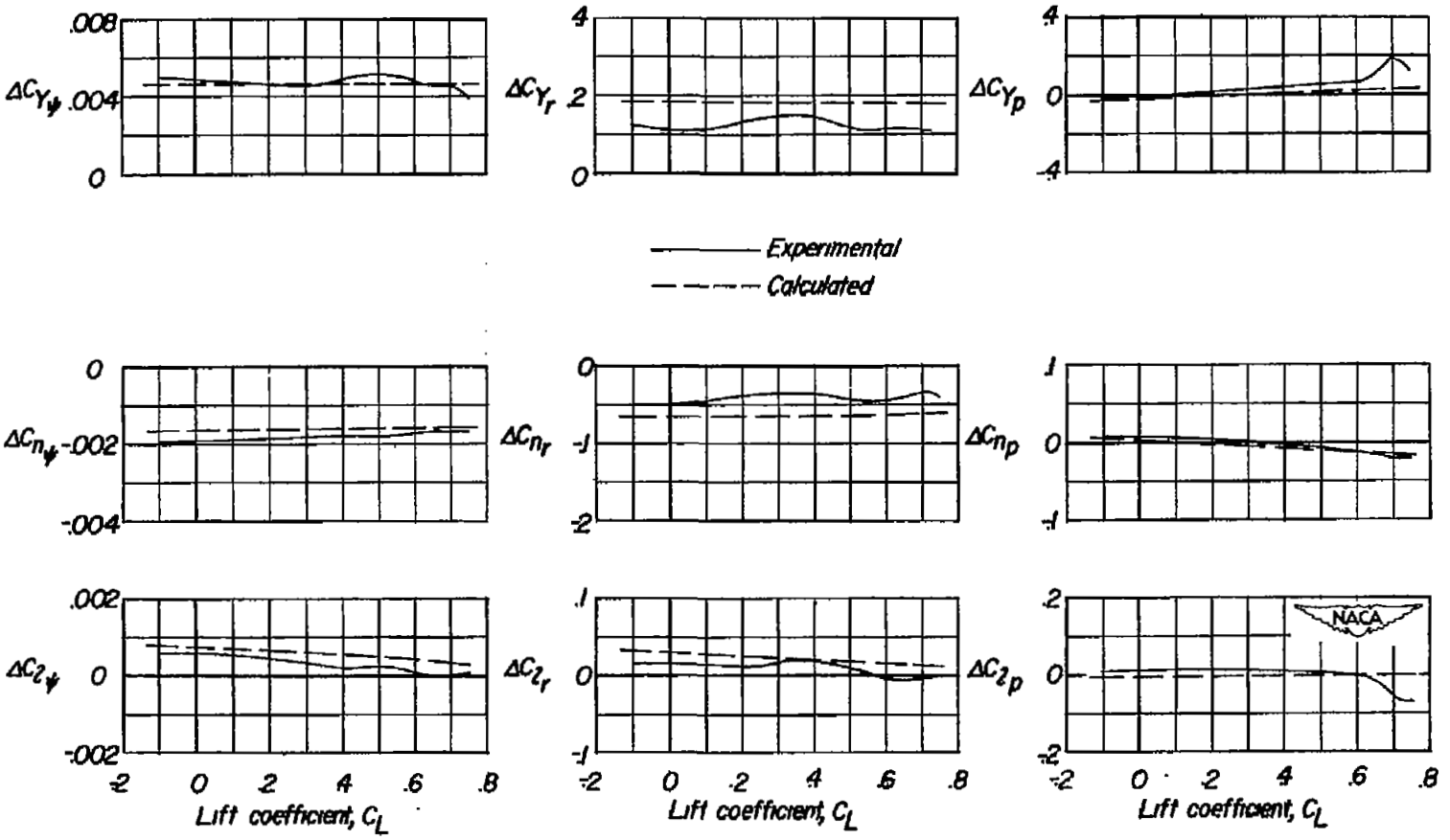

Figure 9.- Increments in the stability derivatives due to the vertical fin in arrangement V(a'L). Calculated increments are based on the theoretical lift-curve slope of the vertical fin.

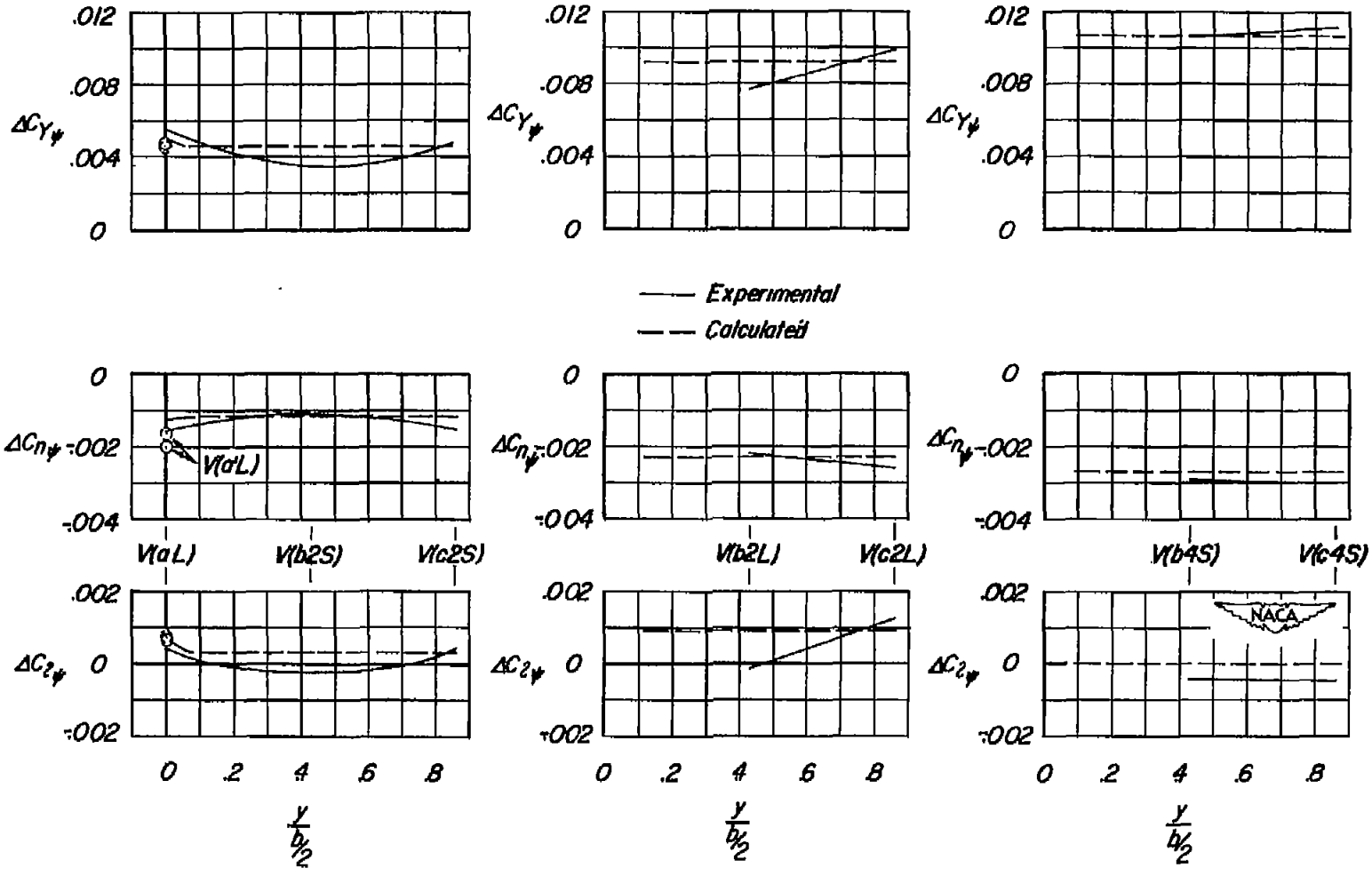

(a) Straight flow.

Figure 10.- The variation with lateral position of the increments to the stability derivatives due to each of the fin arrangements tested. $C_L = 0$.

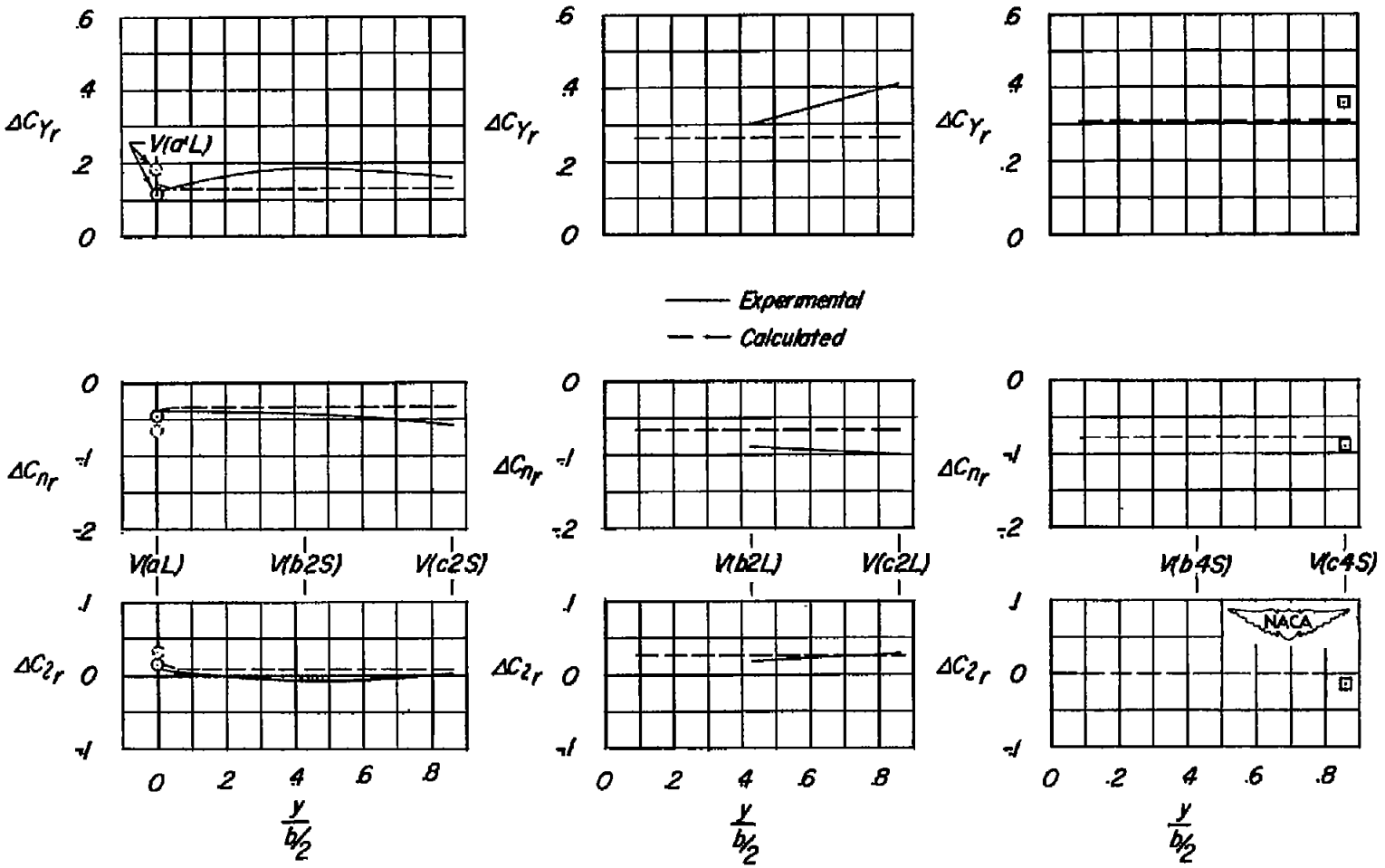

(b) Yawing flow.

Figure 10.- Continued.

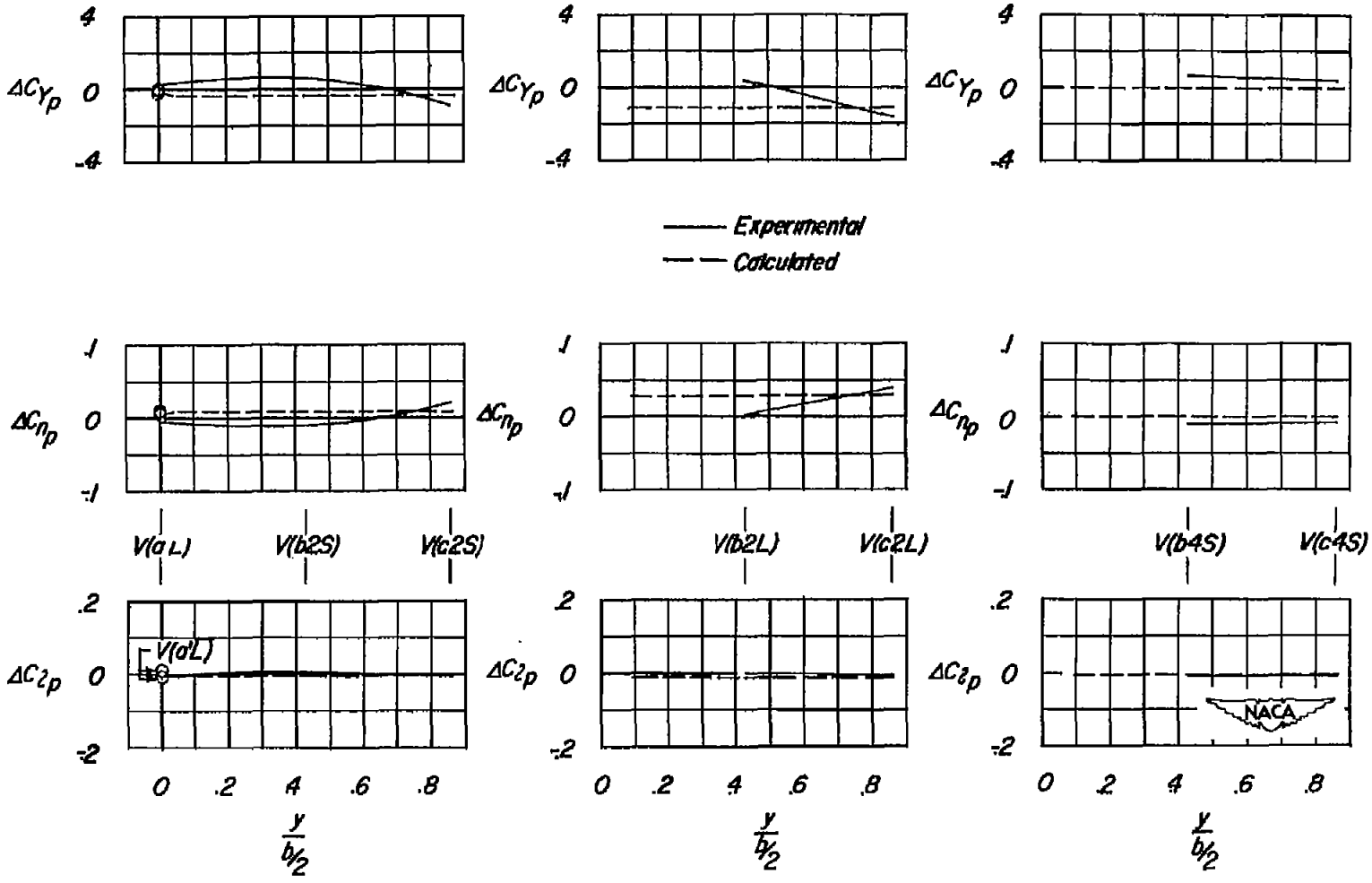

(c) Rolling flow.

Figure 10.- Concluded.